Geochemistry 84 (2024) 126121

Contents lists available at ScienceDirect

Geochemistry

journal homepage: www.elsevier.com/locate/chemer

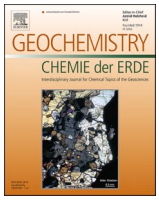

Geochemistry of hydrothermal illitizations in Eocene Kösedağ magmatic rocks, Zara-Suşehri area, NE Sivas, East-Central Anatolia: Origin and age of alteration

Ömer Bozkaya [a,*], Zeynel Başıbüyük [b], Hüseyin Yalçın [c], Gülcan Bozkaya [a], Deniz Hozatlıoğlu [c], Marek Szczerba [d]

[a] Department of Geological Engineering, Faculty of Engineering, Pamukkale University, Denizli, Turkey
[b] Department of Geological Engineering, Faculty of Engineering and Architecture, Ahi Evran University, Kırşehir, Turkey
[c] Department of Geological Engineering, Faculty of Engineering, Cumhuriyet University, Sivas, Turkey
[d] Institute of Geological Sciences, Polish Academy of Sciences, Krakow, Poland

ARTICLE INFO

Handling Editor: Emin Çiftçi

Keywords:
Eocene magmatism
Hydrothermal alteration
Clay minerals
Stable isotope geochemistry
K-Ar dating

ABSTRACT

The study area located at the periphery of the collision zone between the Eurasian plate (i.e. Pontides) and Tauride-Anatolide platform, NE of Sivas in the east-central Turkey, which is part of the Tethyan Metallogenic Belt. Mixed-layer illite-smectite (I—S) and illite minerals are derived within the hydrothermal alteration zones with a few km^2 surface areas (up to 30 km^2) in Eocene volcanic and plutonic rocks. The representative I—S and illite samples taken from plutonic- and volcanic-hosted alteration zones are investigated by optical and scanning electron microscopy (SEM), X-ray diffraction (XRD), major and trace elements and O—H isotope geochemistry and K—Ar dating methods. Different types of hydrothermal alterations, such as propylitic and phyllic alteration in the plutonic rocks and argillic alteration in the volcanic rocks were developed as a result of intrusion of Kösedağ Pluton (syenite) into Karataş Volcanics (basaltic trachy-andesite and trachyte) with relations of hot-hot contact. The main phyllosilicate/clay minerals are characterized by kaolinite and I—S in volcanic-hosted argillic alteration zones, whereas I—S and illite in plutonic-hosted phyllic zones. The ordering types (Reichweite) of I—S and illites are represented by R1 I—S (I = 65–80 % in I—S) + R3 I—S (I = 90 % in I—S) in the volcanic-hosted rocks, and R3 I—S (I = 90 % in I—S) and illite (S = 3–5 %). Dioctahedral ($d_{060} \leq 1.500$ Å) R3 I—S and illites have 1 M_d + 1 M and 1 M_d + 1 M + 2 M_1 polytypes, respectively. The major and trace elements such as TiO_2, Fe_2O_3, MgO, Na_2O, P_2O_5, Sc, V, Cu, Ge, Sr, Hf, Zr and Y increase in the volcanic-hosted I—S, whereas SiO_2, Al_2O_3, K_2O, Pb, W, Mo, As, Sb, Rb and U in the plutonic-hosted I—S and illites. The chondrite-normalized distributions of I—S and illites present a great similarity to those of host rocks. The chondrite-normalized rare earth element (*REE*) concentrations are more enriched in the volcanic-hosted I—S in comparison with the plutonic-hosted I—S and illites having distinctive Eu negative anomaly, which indicate deriving from volcanic matrix and K-feldspar, respectively. Oxygen and hydrogen isotope data of illitic clays indicate that the hydrothermal fluids are originated from magmatic water. According to stable isotopes and fluid inclusion data, I—S and illites were formed at the temperature conditions ~150 °C in volcanic-hosted argillic zone, whereas ~250 °C in plutonic-hosted phyllic zones. K—Ar dating of alunite, I—S and illite minerals indicate that the hydrothermal alteration was started at 40.45 ± 1.28 Ma, almost 2 Ma after the Q-syenite intrusion, within the plutonic body as phyllic alteration stage, and continued up to 35.27 ± 2.81 Ma, with a duration of ~5 Ma, and finalized before the exhumation of the Kösedağ Pluton (28–30 Ma). The geochemical characteristics of I—S and illites were controlled by host-rock, condition, origin, and ages of alterations and they can be used as an important tool for magmatic-hydrothermal systems.

* Corresponding author.
E-mail address: obozkaya@pau.edu.tr (Ö. Bozkaya).

https://doi.org/10.1016/j.chemer.2024.126121
Received 31 January 2024; Received in revised form 14 April 2024; Accepted 17 April 2024
Available online 23 April 2024

1. Introduction

In magmatic-hydrothermal systems, intrusion of magmatic rocks commonly causes hydrothermal alterations involving mineralogical, chemical and textural changes resulting from the interaction of hot aqueous fluids with host rocks. Several types of alterations, i.e., propylitic, phyllic (or sericitic) and argillic are developed in relation to temperature and alkali and hydrogen metasomatism (aK^+/aH^+) (Pirajno, 2009). Alteration-related clay/phyllosilicate minerals (e.g., kaolinite, pyrophyllite, illite, mixed-layered illite-smectite, smectite) are successfully used to determine the low-temperature conditions of ore formations (e.g., Millot, 1970; Velde, 1977; Inoue, 1995; Pirajno, 2009). The hypogene clay/phyllosilicate minerals, kaolinite, pyrophyllite, illite, I—S and smectite, are considered to preserve their original hydrothermal signatures (Sheppard and Gilg, 1996). In addition to crystal-chemical properties of clays (illite crystallinity, polytype and d_{060}), geochemical (major and trace elements, stable and radiogenic isotopes) data can also provide significant information about the alteration conditions including temperature, origin and age of ore-forming fluids (e.g., Inoue and Kitagawa, 1994; Inoue, 1995; Bechtel et al., 1999; Tillick et al., 2001; Yan et al., 2001; Zwingmann et al., 2004; Bozkaya et al., 2016, 2019a, 2019b).

Epithermal alterations related to high acidic solutions in association with the high H+ metasomatism and acidic environment at temperatures between 100 and 300 °C cause the degradation of aluminum silicates and subsequent silica enrichment that give rise to development of silica-rich argillic alteration zones, which is characterized by the formation of silica, clay/phyllosilicate and sulphate minerals (e.g., opal, opal-CT, quartz, halloysite, kaolinite, dickite, pyrophyllite, alunite and jarosite). Thus, the argillic alteration zone is divided into sub-mineral associations as silica, alunite, alunite-kaolin and kaolin group, respectively, from extreme acidic (low pH) conditions to neutral (low-intermediate pH) conditions (e.g., Corbett and Leach, 1998). Clay/phyllosilicate occurrences associated with hydrothermal alteration are important not only for their scientific meaning, but also for the formation of clay deposits that can be used as industrial raw materials (e.g., Inoue, 1995; Dill et al., 1997, 2000; Ece et al., 2008, 2013).

The study area located at the periphery of the collision zone between the Eurasian plate (i.e. Pontides) and Tauride-Anatolide platform, south of the North Anatolian Fault Zone (NAFZ), NE of Sivas in the east-central Turkey (Fig. 1), is representing the convergent plate margin setting in the Alpine-Himalayan system. East-central Turkey is part of the Tethyan Metallogenic Belt (Yiğit, 2012) or the western extension of the Tethyan Eurasian Orogenic Belt (Mao et al., 2014), and has a complex geologic and tectonic history due to the collision of different continental fragments and their amalgamation after the convergence of the Anatolide-Tauride platform (Gondwana) and the Pontides (Laurasia) during the Mesozoic-Cenozoic Eras (Fig. 1a, Şengör and Yılmaz, 1981; Kuşcu et al., 2013).

Hydrothermal alteration is completely associated with the Eocene magmatic (plutonic and volcanic) rocks and did not affect the Miocene volcanic and sedimentary cover rocks. The Eocene magmatism begins with pyroclastic products (Akıncılar formation), and continues with basaltic-trachytic lava flows (Karataş Volcanics), and ends with syenite (Kösedağ pluton) at shallow depths (Başıbüyük, 2006; Başıbüyük and Yalçın, 2019). The intrusion of the Kösedağ pluton into Karataş volcanics caused the widespread hydrothermal alterations (pyropilitic, phyllic/sericitic and argillic) which affected both pluton and volcanic rocks. The hydrothermal minerals are mainly represented by quartz, opal-CT, kaolinite, pyrophyllite, illite, mixed-layered illite-smectite (I—S) and smectite as early stage, and barite, alunite, goyazite, jarosite, chlorite and mixed-layered chlorite-smectite (C—S) as late stage of hydrothermal processes (Başıbüyük, 2006; Başıbüyük and Yalçın, 2019).

The aim of this study is to investigate the geochemical and fluid inclusion characteristics of hydrothermal illite/I-S and quartz minerals associated with the intrusion of syenitic pluton into basaltic-trachytic volcanic rocks. In this context, hydrothermal alteration characteristics (temperature condition, origin of mineral-forming fluids, age of alteration, etc.) of the plutonic- and volcanic-hosted alteration zones will be explained based on the detailed geochemical (major, trace element compositions, O and H isotopes, K—Ar dating) and microthermometric (homogenization temperature, fluid composition, salinity) data.

2. Stratigraphy and lithology

The basement unit in the study area is Upper Cretaceous-Paleocene Refahiye complex (Yılmaz et al., 1985) composed of serpentinized peridotites and serpentinites (Fig. 2). The Eocene magmatism started with the pyroclastic eruptions which deposited as intercalations of volcanic breccias, agglomerate and tuffite within the siliciclastic and carbonate rocks of the Akıncılar Formation. Eocene magmatism continued with basaltic-trachytic lava flows of the Karataş Volcanics and ended with the intrusion of the Kösedağ Pluton.

Karataş Volcanics vary in composition from basaltic trachy-andesite to trachyte, and are generally massive and partly contain thick lava flow structure. The fresh (unaltered) parts of volcanics are greenish black and brown-purple in color, and occasionally contain distinct crack systems (Fig. 3a). The Karataş Volcanics exhibit hot-hot contact relation with the Kösedağ Pluton at shallow depths. The altered parts of volcanics are light brown-yellow-white in color, and exhibit porphyritic texture containing coarse grained feldspar (0.5–3 cm) and pyroxene phenocrysts close to the Kösedağ Pluton (Başıbüyük, 2006; Başıbüyük and Yalçın, 2019). The formation of coarse-grained phenocrysts is probably related to the emplacement of the pluton, especially the formation of late-stage pegmatitic biotite syenites.

The Kösedağ pluton with pinkish to brick red colors (Fig. 3c) consists of syenites and quartz syenites with a phaneritic, porphyritic texture characterized by K-feldspar megacrysts set in a coarse- to medium-grained groundmass comprising K-feldspar, plagioclase, clinopyroxene, amphibole, biotite and quartz (Boztuğ, 2007). Whole rock Rb—Sr and zircon U—Pb age determination from quartz syenite reveals that it was emplaced into volcanic rocks (Karataş Volcanics) between 45 and 42 Ma (Kalkancı, 1974, 1978; Eyuboglu et al., 2017), whereas Rb-Sr ~ 37 Ma age was also determined for pegmatitic biotite syenites (Kalkancı, 1974, 1978). The Kösedağ pluton could have been derived from partial melting of a metasomatized mantle layer which was accreted into the collision zone between the Eurasian plate and the Tauride-Anatolide platform along the İzmir-Ankara-Erzincan suture zone (Eyuboglu et al., 2017). A post collisional extensional regime, induced by slab break-off following the continent-continent collision, may have melted these metasomatized mantle slices to produce the high-K, alkaline, metaluminous magma source of the Kösedağ pluton (Boztuğ, 2007). Apatite fission track age versus elevation profiles and temperature-time-path modeling of the Eocene Kösedağ pluton indicate an Oligocene (28–30 Ma) rapid exhumation (Boztuğ and Jonckheere, 2007).

Eocene and older units were unconformably covered by Miocene-Pliocene clastic, carbonate and volcanic rocks (Başıbüyük, 2006). Early Miocene Onarı formation has basal conglomerate, limestone and claystone with thick gypsum interlayers (Ibikkaya member) at the lower parts, sandstone, conglomerate and limestone at the upper parts (Kızık member). Late Miocene-Pliocene andesitic-dacitic (İsola Volcanics) and basaltic (Şerefiye Basalt) rocks cut the Eocene magmatic and Early Miocene clastic rocks (Fig. 2). Pliocene conglomerate, sandstones with claystone and carbonate rocks (Kadıköy Formation) and Quaternary alluviums unconformably covers the older units.

3. Materials and methods

A total of 5 pure (mono-mineral) clay samples (two illite, three I—S), obtained from clay mineral separation (<2 μm), from volcanic- and plutonic-hosted alteration zones were selected from previously investigated samples in the study area (Başıbüyük, 2006). I—S and illite

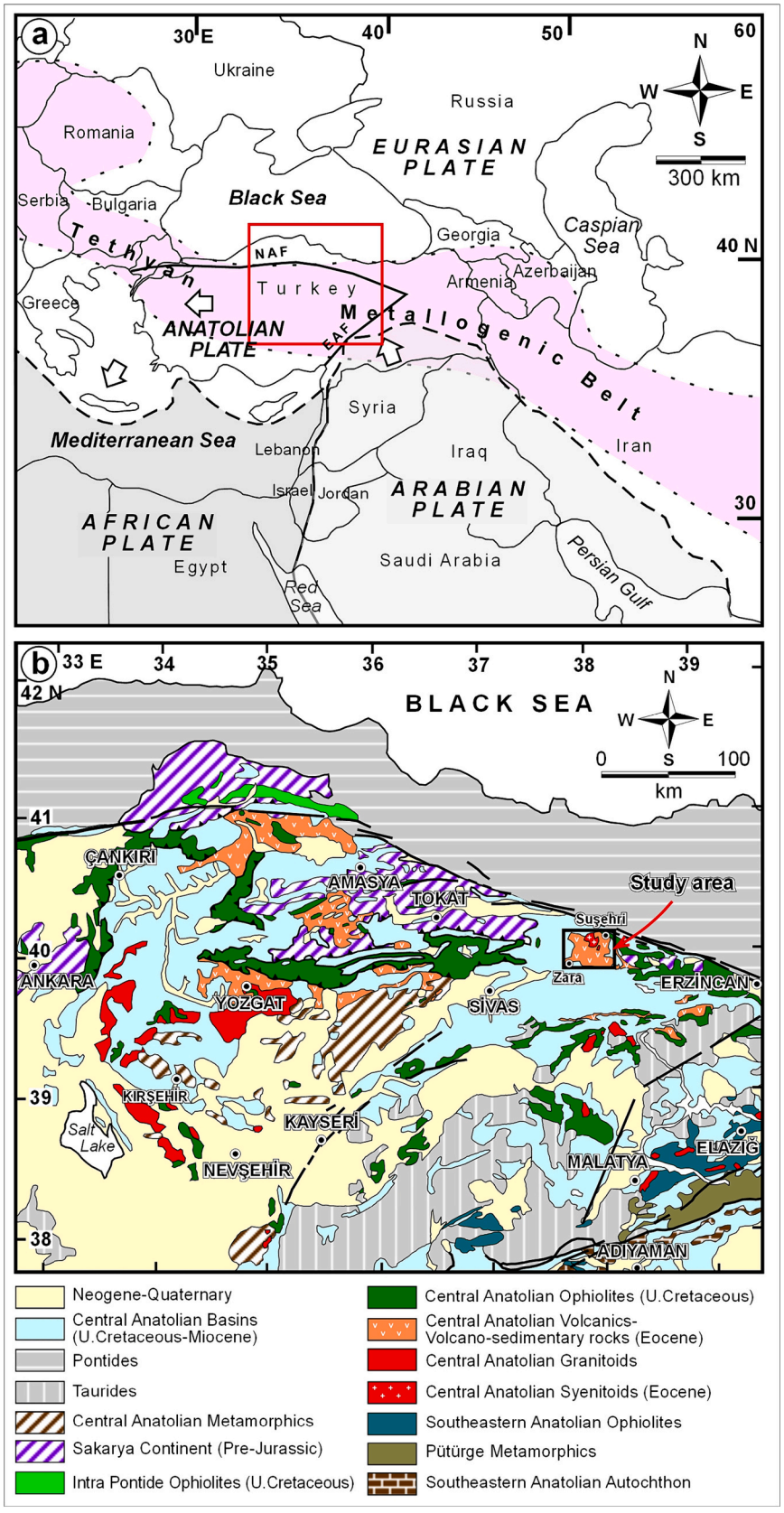

Fig. 1. (a) Location of the East-Central Anatolia in relation to the boundaries of the major tectonic plates and Tethyan Metallogenic Belt (Yiğit, 2012), NAF: North Anatolian Fault, EAF: East Anatolian Fault, (b) The regional geological map of the study area (Bingöl, 1989; Görür et al., 1998).

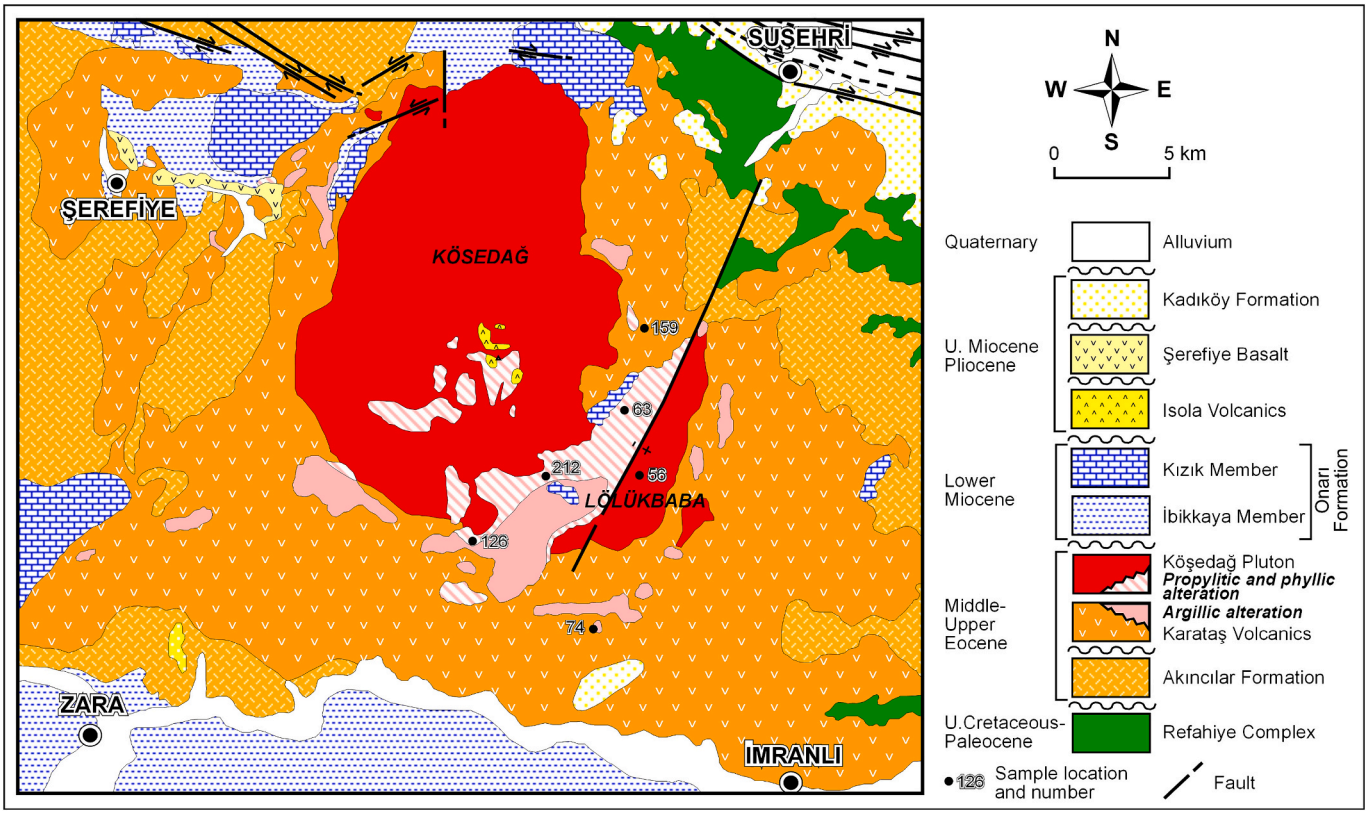

Fig. 2. Geological map of the study area (Kalkancı, 1974; Yılmaz et al., 1985; Uysal et al., 1995; Başıbüyük, 2006).

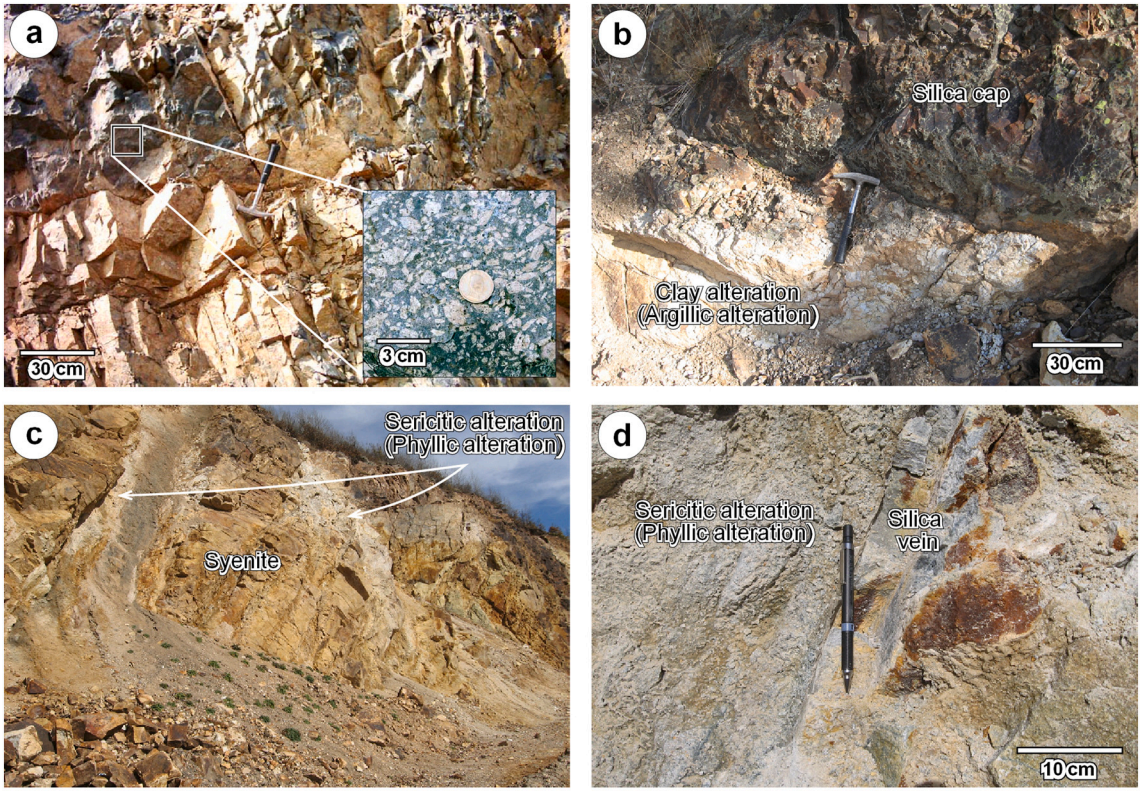

Fig. 3. Field photographs of hydrothermal alterations in the study area, a) porphyritic texture in the Karataş volcanics, b) White clay alteration and silica cap at the upper parts of the volcanic-hosted argillic alteration zone, c) White-light gray sericitic (phyllic) alteration zones within the light brown-yellowish white syenites of the Kösedağ Pluton d) Silica veins within the plutonic-hosted phyllic zones. (For interpretation of the references to color in this figure legend, the reader is referred to the web version of this article.)

minerals were chosen because they are useful as mineralogical and geochemical indicators of hydrothermal processes, as well as because their formation ages can be determined. The investigation methods of optical and electron microscopy, major and trace element geochemistry and stable isotope data were previously reported from Başıbüyük (2006). Since this study (PhD thesis) has not been published, the investigation methods are given again below. K—Ar dating of illite/I-S minerals and computer-based program applications (NEWMOD, WILDFIRE and WINFIT) were carried out during this study.

Textural and mineralogical features of host and altered rock samples were conducted by transmitted light microscopy. In addition, the secondary electrons (SE) images of gold-coated fragments were examined by scanning electron microscopy (SEM) with a JEOL JSM-6490 instrument equipped with IXRF energy dispersive spectrometry (EDS) system at the Turkish Petroleum Corporation in Ankara, Turkey. Operating conditions were 32 s counting time and 20 kV accelerating voltage.

Geochemical (major, trace/REE and O—H stable isotopes) and additional mineralogical (X-ray diffraction) analysis were performed on host-rocks and extracted pure clay samples. The geochemistry data of unaltered volcanic and plutonic host rocks were also used for comparison to geochemistry of illite and I—S. Two samples (illite and I—S) from volcanic- and plutonic-hosted alteration zones were analyzed for illitization age by K—Ar dating method.

The determination of illite and smectite percentages in I—S minerals and polytypes of illites were investigated on geochemically analyzed samples. The computer-based programs, NEWMOD© (Reynolds Jr., 1985) and WILDFIRE© (Reynolds Jr., 1994), were used for illite and smectite ratios in I—S and determination of polytype percentages of illites, respectively. The decompositions of composed peaks for different interstratification types in I—S were distinguished using the WINFIT software program (Krumm, 1996), which reconstructed single peaks by fitting the envelope curve of overlapping peaks.

The chemical compositions and the hydrogen- and oxygen-isotopic compositions of pure illite and I—S clay fractions were determined using a Thermo Jarrell-Ash ENVIRO II ICP, a Varian Vista 735 inductively coupled plasma (ICP) spectrometer, a Perkin-Elmer SCIEX ELAN Model 6000, 6100, or 9000 inductively coupled plasma-mass spectrometer (ICP-MS), or a Finnigan MAT 250 mass spectrometer at the ACTLABS Activation Laboratory, Ltd. (Ancaster, Ontario, Canada).

Samples were prepared and analyzed in a batch system for major and trace elements, mixed with a flux of lithium metaborate/tetraborate, and fused in an induction furnace. The melt was immediately poured into a solution of 5 % HNO_3 containing an internal standard and mixed continuously until completely dissolved (~30 min).

For analysis of $^{18}O/^{16}O$ isotopic ratios, samples were reacted with BrF5 at~6 50 °C in nickel bombs following the procedures described by Clayton and Mayeda (1963). The fluorination reaction converts O in the minerals to O_2 gas, which is subsequently converted to CO_2 gas using a hot C rod. For D/H isotope ratios, samples weighing 0.02 to 1.0 g were wrapped in molybdenum foil and placed in a platinum crucible, which was then suspended inside a quartz extraction vessel. The vessel and its contents were out gassed in a vacuum at 120 °C for 4 h to remove surface-adsorbed water. The sample was then heated inductively at 1400 °C for up to 20 min and the gases collected in a trap held at −196 °C. Nearly all of the hydrogen was thus released in the form of water, but miniscule quantities of hydrocarbons or molecular hydrogen released or produced during this treatment were oxidized over CuO at 55 0 °C to form H_2O and CO_2, which were also collected in the trap. The accumulated water, representing the total amount of hydrogen in the samples, was separated from the other gases by differential freezing techniques. The water was reacted with uranium at 900 °C to produce H_2 and collected on charcoal at −196 °C. The O—H isotopic data are reported in the standard delta notation as per mil deviations from V-SMOW.

The K—Ar dating of illite and I—S samples was performed in Institute of Geological Sciences, Polish Academy of Sciences (Poland). The potassium contents were measured using Sherwood Model 420 flame photometer on two portions of HF dissolved samples, in order to increase precision. After the reaction with HF, the samples were dissolved in diluted HCl and proceeded to photometric measurements. Radiogenic argon measurements were performed on Nu Instruments Noblesse multi collector noble-gas spectrometer (NG039). Each sample was wrapped in tantalum foil and melted by defocused 972 nm infrared laser. CuO added to the samples enhances oxidation of organic matter during this step. Titanium sublimation and Z-100 (SAES Getters) getter pumps were used for cleaning the extracted gases. The amount of aliquot of ^{38}Ar, used as the spike, was determined by measuring international standard GL-O (Odin, 1982). Age errors were calculated from the law of error propagation, taking into account uncertainties of spectrometric measurement of argon isotopes, weighting, potassium measurements, normalization of amount of ^{38}Ar in spike based on dating of GL-O standard and assessment of $^{40}Ar/^{36}Ar$ and $^{40}Ar/^{38}Ar$ ratios, measured every day for air aliquots.

4. Results

4.1. Field characteristics

Three types of hydrothermal alterations (propylitic, phyllic/sericitic and argillic) were identified within the Kösedağ Pluton and Karataş Volcanics and their textural and mineralogical characteristics were previously given by Başıbüyük (2006). Hydrothermal clay/phyllosilicate mineral occurrences are located along the circular tension fractures within the volcanic rocks, distributed parallel to the contact of plutonic body and volcanic rocks, and also within the plutonic body along the fault zone with NE-SW direction. Hydrothermal alterations zones are usually observed as a few km^2 surface areas and are distinguished by the silica cap consisting of iron oxide (goethite) and silica minerals in the uppermost parts.

The distributions of propylitic alteration zones developed as a few-meter zones within the volcanic rocks along the contact of plutonic-volcanic bodies. In the propylitic alteration zones, plutonic rocks are observed as pinkish color with fine-grained holocrystalline texture, whereas volcanic rocks displays grayish green color with porphyritic texture (Başıbüyük and Yalçın, 2019).

Argillic alteration exhibits wide distributions in the study area. It is usually developed in volcanic rocks and rarely observed in plutonic body as small-scale occurrences. Hydrothermal clay (kaolinite, I—S), sulfate (alunite) formations overlain by brecciated ferrous silica cap and silica-rich iron oxidized zones at the uppermost parts (Fig. 3b). The yellowish-white kaolinite-rich alteration zones are common in argillic alteration zones. Volcanic host rocks were pervasively altered and rarely unaltered primary volcanic rocks were remained as small-scale (1–2 m) areas (Başıbüyük and Yalçın, 2019).

Phyllic/sericitic alterations have been extensively developed in the Kösedağ Pluton and observed as light green-yellow color with a thickness reaching up to 10 m (Fig. 3c-d). They include barite and tourmaline veins together with goethite, jarosite which are developed along the fracture zones.

4.2. Petrography

Optical microscopic investigations of the highly altered volcanic rocks in the argillic alteration zones show that the primary porphyritic texture is still preserved and feldspar phenocrysts can only be identified by their shapes due to complete kaolinitization and sericitization, i.e. illitization (Fig. 4a-b). The microliths and volcanic glass in the matrix completely were also transformed into clay minerals. Kaolinite, replacing feldspar phenocrysts, can be easily recognized by the interference color, whereas I—S displays very fine mica-like flakes with high birefringence (Fig. 4a-b). In the altered syenites, feldspar minerals are completely sericitized, and hydrothermal silica minerals are

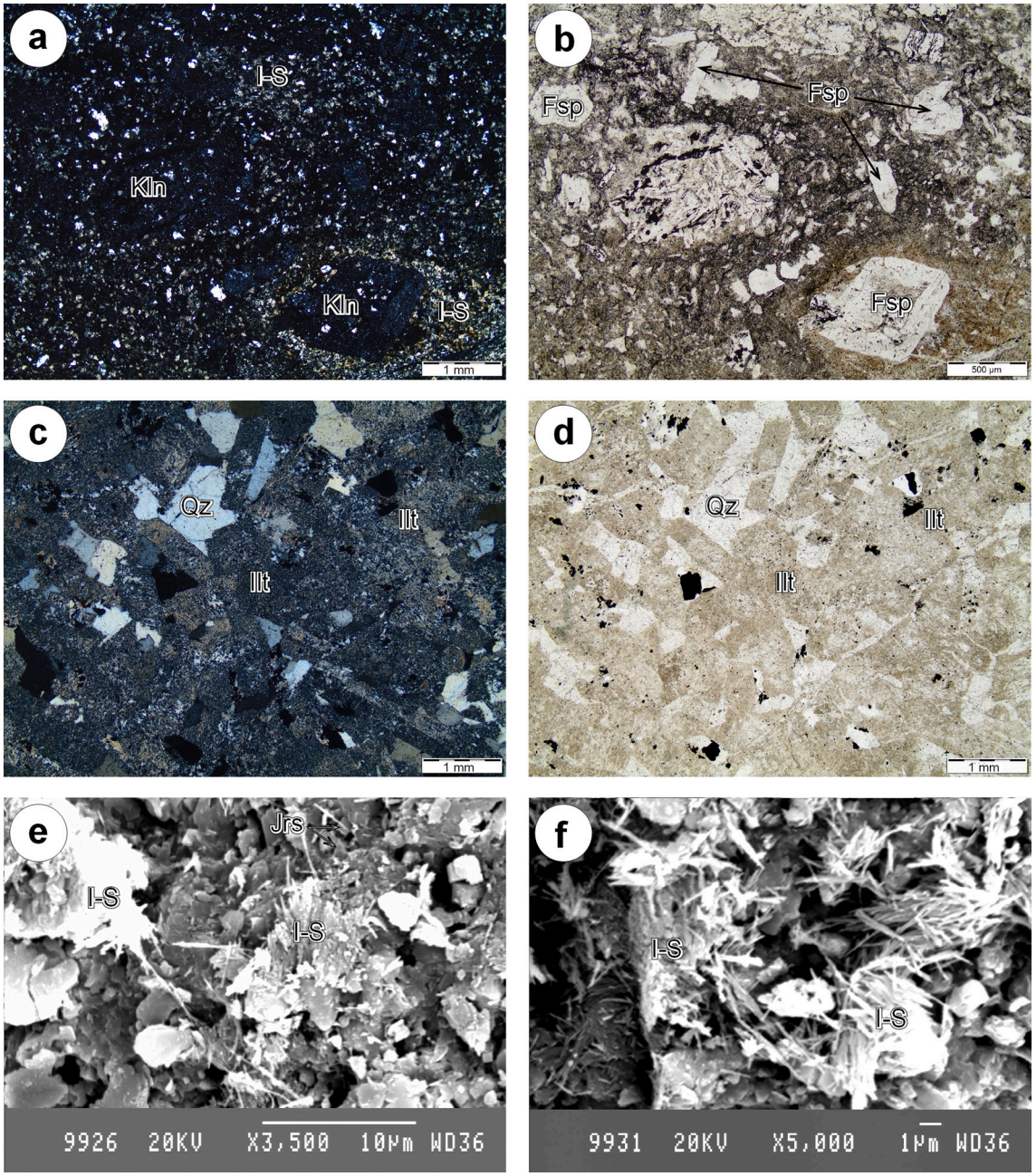

Fig. 4. a-b) Optical photomicrographs of pseudomorphs of feldspar phenocrysts (Fsp) replaced by kaolinite (Kln) and mixed-layered illite-smectites (I—S) within the volcanic matrix (a: crossed nicols-cn, b: plane-polarized light-ppl), c-d) Pseudomorphs of feldspar phenocrysts (Fsp) replaced by illites (Ilt), and hydrothermal quartz in altered syenite sample (c: cn, d: ppl), e-f) SEM photomicrographs of fibrous/acicular I—S minerals in altered syenite sample.

precipitated among the feldspar crystals (Fig. 4c-d).

According to scanning electron microscope (SEM) investigation of an altered volcanic rock sample, hydrothermal I—S minerals are observed as fibrous-acicular minerals, 1–5 μm long, forming parallel bundles in places (Fig. 4e-f). In some places, anhedral quartz, subhedral platy kaolinite and fine-grained (1–2 μm) cubic jarosite crystals (Jrs) are associated to I—S crystals.

4.3. Mineralogy

Hydrothermal alteration related minerals in the study area are classified as phyllosilicate/clay (kaolinite, illite, smectite, chlorite, I—S, C—S and pyrophyllite), oxide and hydroxide (hematite and goethite), carbonate (calcite, dolomite), sulphate (barite, alunite and jarosite), phosphate (goyazite) and silica (quartz and opal-CT) minerals (Başıbüyük and Yalçın, 2019). Chlorite, sericite (illite), calcite and epidote and iron oxides were developed in the fractures and matrix of the altered andesites in the propylitic zones. The most common hydrothermal mineral assemblages in the volcanic-hosted argillic zones are kaolinite + I-S + quartz + goethite + goyazite, kaolinite + I-S + quartz + alunite + goethite and kaolinite + I-S + quartz + jarosite + feldspar ± goethite and/or goyazite. Whereas, illite + I-S + quartz + jarosite ± goethite ± feldspar and illite + I-S + quartz + feldspar are determined as alteration mineral assemblages in plutonic-hosted phyllic alteration zones (Başıbüyük and Yalçın, 2019).

XRD oriented clay patterns of the samples investigated within the scope of this study are given in Table 1 and Fig. 5. Volcanic-hosted clay samples from argillic alteration zones (ZK-74 and ZK-159) are made up

Table 1
Mineralogical characteristics of the investigated samples.

Sample no	Host rock and alteration zone	Whole rock (%)					Clay fraction (%)			d_{060} (Å)	Illite (%) in I-S	Illite polytype		
		Quartz	Feldspar	Jarosite	Alunite	Clay	Illite	I-S	Kln			$2M_1$	1 *M*	1 M_d
ZK-63	Plutonic-hosted phyllic zone	42	06	–	–	52	100	–	–	1.498		05	10	85
ZK-126		30	–	07	–	63	–	100	–	1.498	90	–	10	90
ZK-212		45	–	–	03	55	100	–	–	1.497		05	10	85
ZK-74	Volcanic-hosted argillic zone	31	–	05	03	61	28	70	02	1.500	85			
ZK-159		08	05	08	–	79	20	80	–	1.500	85			

I—S and illite minerals with negligible amounts of kaolinite. The illite + I—S (I85%-S15%) patterns calculated by NEWMOD (Reynolds Jr., 1985) completely fit both the air-dried and glycolated patterns of the sample ZK-74. WINFIT-decomposition of XRD peaks between 2θ 4 and 10° in the sample ZK-159 indicate that the presence of two types of I—S (R3: I_{90}-S_{10} and R1: I_{70}-S_{30}) and illite phases (Fig. 5). Plutonic-hosted clay samples from phyllic alteration zones are represented by two illites (ZK-63 and ZK-212) and one R3 I—S (ZK-126) and indicate relatively higher illite contents (>90 %) rather than those of volcanic-hosted clay samples (Figs. 5 and 6). Illite Kübler index (KI = 0.64–0.66 Δ°2θ) and crystallite thickness ($N = 70$ Å) values of illites point out the high-grade diagenetic condition, possible temperature range between 100 and 200 °C, assuming for sedimentary-diagenetic environments (Frey, 1987; Merriman and Frey, 1999; Ferreiro-Mahlmann et al., 2012). Expandable (or swelling) components and crystallite size of illites were evaluated in the illite KI vs peak intensity ratio (Ir, Środoń, 1984) diagram, in which the mean XRD scattering domain sizes and contents of swelling (smectitic) layers in illites were estimated using the NEWMOD-based graphs (KI vs. Ir) calculated by Eberl and Velde (1989). The swelling components (smectite) and XRD scattering domain sizes (nanometer-nm) of the illites are 3 to 5 % and 15 to 20 nm for ZK-63 and ZK-212 samples, respectively.

According to the WILDFIRE (Reynolds Jr., 1994) calculated patterns of illite polytypes, R3 I—S has 1 M_d (90 %) + 1 *M* (10 %), whereas illites have 1 M_d (85 %) + 1 *M* (10 %) + 2 M_1 (5%) polytypes (Fig. 6). WINFIT decomposition of peaks of the unoriented XRD patterns referring to 1 *M* and 2 M_1 polytypes are also illustrated. I—S and illites have dioctahedral composition ($d_{060} \leq 1.500$ Å).

4.4. Fluid inclusion characteristics

Fluid inclusion studies have been carried out on plutonic- and volcanic-hosted hydrothermal quartz as veins and silica roof and plutonic-hosted hydrothermal barite as veins. The field and optical microscopic observations indicate that silica and barite occurrences are directly related to hydrothermal fluids which caused the clay mineral occurrences. On the basis of petrographic characteristics and microthermometric behaviors of FIs, three types of fluid inclusion were identified: (1) primary inclusions in quartz crystals, (2) secondary inclusions occurred in trails along healed fractures in quartz and (3) primary inclusions in barite. In addition to common bi-phase (liquid+vapor) inclusions, mono-phase (vapor) and (liquid) are also observed. There are various sizes (mostly <5–10 mμ) and shapes (rounded, semi-rounded and tabular) for fluid inclusions.

The salinity of fluids shows differences for different rock types: 13.8 to 20.5 (avg.16.4) wt% NaCl equiv. for galena-bearing quartz veins, 9.8 to 16.9 (avg.14.9) wt% NaCl equiv. for plutonic-hosted quartz veins and 10.7 to 15.3 (avg. 13.1) wt% NaCl equiv. for plutonic-hosted barite veins.

The average homogenization temperatures are measured as 307.7 °C and 148.7 °C for primary and secondary inclusions within the plutonic-hosted galena-bearing quartz veins. The average homogenization temperatures of 276.8 °C, 148.8 °C and 268.3 °C are determined for primary inclusions in plutonic- and volcanic-hosted quartz and plutonic-hosted barite occurrences, respectively. Plutonic-hosted hydrothermal quartz minerals show relatively higher temperature and salinity values with respect to those of volcanic-hosted quartz minerals.

4.5. Geochemistry

4.5.1. Major-elements

Chemical compositions and structural formulae of volcanic- and plutonic-hosted I—S and illites are given in Table 2. The chemical compositions of fresh (unaltered) volcanic- and plutonic-host rocks were also given for comparison. The structural formulae of illite and I—S were calculated on the basis of 22 negative charges corresponding to 10 oxide and two hydroxide ions (Weaver and Pollard, 1973).

The tetrahedral substitutions of 0.38 to 0.67 atoms of Al for Si, and octahedral substitutions of 0.07 to 0.15 atoms of Fe and 0.06 to 0.19 atoms of Mg for Al were determined per formula unit (a.p.f.u.) (Table 2). The total number of octahedral cations is 1.94–2.00. The sum of octahedral Al and Ti is 1.51–1.83 and 0.01–0.11 a.p.f.u., respectively. The major interlayer cation is K (0.44–0.68 a.p.f.u.). Ca and Na from other interlayer cations have relatively small values (0.01–0.09 a.p.f.u.). Interlayer Na increases in I—S. According to theoretical muscovite composition (the a.p.f.u. of interlayer K = 1 and octahedral Al = 2), the numbers of tetrahedral and octahedral substitutions are related to smectite components which vary between 32 and 56 % with respect to the K atom numbers of I-S; this state was confirmed by total interlayer charge values of 0.61–0.71 eq/formula unit.

In the tetrahedral charge vs. octahedral charge ternary diagram (Fig. 7a), both R1 and R3 types of I—S and illites fall within the theoretical I—S area between smectite and illite, indicating that tetrahedral charge changes from 0.6 to 0.8 eq/formula unit. I—S and illite structural compositions are distributed from pyrophyllite to muscovite near illite point on the Si vs. Na + K compositional diagram (Fig. 7b). I—S minerals are closer to the pyrophyllite corner, whereas illites are found near the illite field. In other words, I—S and illites were separated in the diagram.

The volcanic-hosted clays (R1 and R3 types of I—S) have relatively lower SiO_2, Al_2O_3 and K_2O concentrations and higher TiO_2, Fe_2O_3, MgO, Na_2O and P_2O_5 concentrations than those of plutonic-hosted clays (illites and R3 type of I—S) (Fig. 8a). When compared host-rock and clay compositions, SiO_2, Al_2O_3, MgO and K_2O values are close to each other, but Fe_2O_3, MnO, CaO and Na_2O values of clays are lower than those of host-rocks (Fig. 8b). Host-rock normalized concentrations of SiO_2, Al_2O_3, Fe_2O_3, MgO and K_2O of volcanic- and plutonic-hosted clays are close to each other. MnO and CaO concentrations of volcanic-hosted clays have lower concentrations than the plutonic-hosted clays, but have higher concentrations of TiO_2, Na_2O and P_2O_5 than plutonic-hosted clays.

4.5.2. Trace-elements and REE

Trace-element concentrations, including *REE*, of host-rocks and hydrothermal clays are given in Table 3. Trace and *REE* element compositions of host-rocks and clays are similar to each other. The plutonic host- rock is richer in Pb, Zn, W, As, Sb, Rb, Tl, Ga, Th and U, and poorer in Cr, Ni, Co, Sc, V, Sr, Zr and Y on comparison to volcanic host-rocks (Fig. 9a). Plutonic-hosted clays have greater values of Pb, Zn, Bi, W, Mo, As, Sb, Ag, Cs, Tl, Ga, Ta, Th and U than those of volcanic-hosted clays (Fig. 9b). According to the chondrite-normalized distributions,

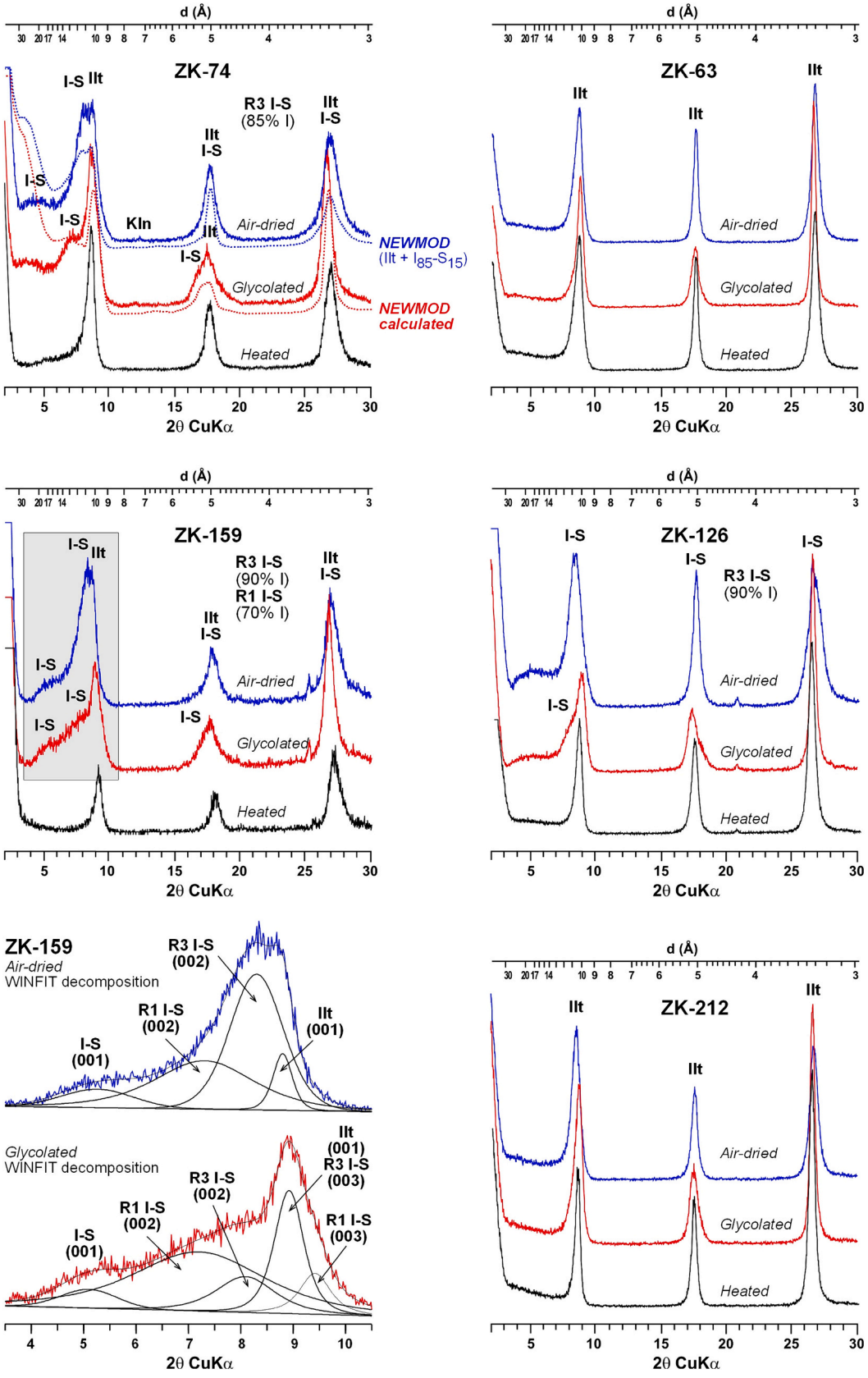

Fig. 5. X-ray diffraction clay fraction patterns of representative samples taken from volcanic- (ZK-74 and ZK-159) and plutonic-hosted (ZK-63, ZK-126 and ZK-212) alteration zones and peak decomposition of sample ZK-159 by using WINFIT program. Ilt = Illite, I-S = Mixed-layered illite-smectite, Kln = Kaolinite.

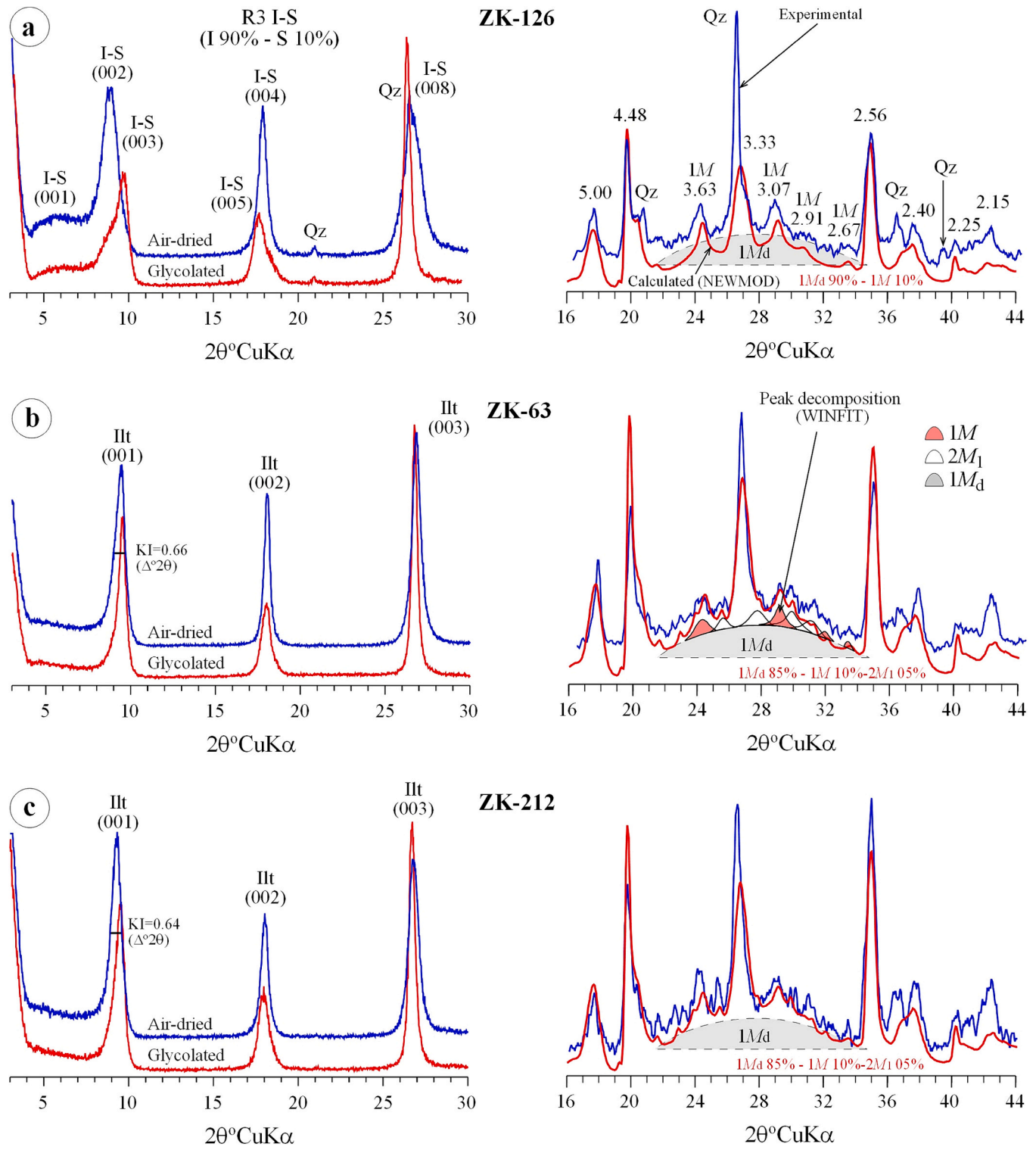

Fig. 6. a) 1 M_d (90 %) + 1 *M* (10 %) polytype association of I—S determined from comparison to WILDFIRE calculated pattern, b-c) 1 M_d (90 %) + 1 *M* (5 %) + 2 M_1 (5%) polytype associations of illite by WILDFIRE method. WINFIT peak decomposition was also shown for confirming the peaks belong to $2M_1$ and 1 *M* polytypes. The XRD patterns in the left part present oriented clay samples and the right part presents unoriented powder clay samples.

host-rocks and clay minerals display similar values each other (Fig. 9c). All samples are enriched relatively to chondrite, and Nb, P and Ti present negative anomalies. Volcanic-hosted clays have an enrichment of up to 20 times (except Rb, Th, U, K and Ta) compared to plutonic-hosted clays. Volcanic- and plutonic-hosted clays are clearly distinguished in the normalized trace element patterns according to host rock compositions (Fig. 9d). Volcanic-hosted clays are enriched compared to the volcanic host-rock, while plutonic-hosted clays depleted with respect to plutonic host-rock.

Chondrite normalized *REE* patterns of Karataştepe volcanics, Kösedağ syenite and hydrothermal clays are given in Fig. 10a. The clay minerals in the studied samples exhibit a broad range of total *REE* abundances, from 50 to 258 ppm (see Table 3), which increase in volcanic-hosted clays. In general, the patterns exhibit similar trends, and

Table 2
Major element compositions (wt%) of magmatic host rocks and clay minerals and structural formulae of I—S and illites (n = number of samples).

Sample	Karataş Volcanics	Kösedağ Q-Syenite	I-S (Volcanic-hosted)		Illite (Plutonic-hosted)		
	Average (n = 4)	ZK-56	ZK-74	ZK-159	ZK-63	ZK-126	ZK-212
SiO_2	55.26	58.73	48.25	50.98	51.74	54.74	52.35
TiO_2	0.829	0.704	0.625	2.121	0.164	0.160	0.167
Al_2O_3	19.29	18.06	29.55	24.91	29.60	27.14	30.69
ΣFe_2O_3	6.64	4.63	2.81	2.95	2.23	1.90	1.51
MnO	0.091	0.123	0.006	0.016	0.053	0.016	0.008
MgO	1.97	0.85	0.92	1.85	1.16	1.02	0.62
CaO	4.76	2.54	0.11	0.22	0.19	0.28	0.08
Na_2O	3.86	4.69	0.67	0.59	0.10	0.05	0.16
K_2O	4.39	6.13	5.33	5.07	8.03	6.65	7.61
P_2O_5	0.43	0.30	0.42	0.46	0.06	0.08	0.07
LOI	2.65	2.01	10.36	9.86	6.99	8.31	7.04
Toplam	100.170	98.767	99.051	99.027	100.317	100.346	100.305
Si			3.33	3.50	3.43	3.62	3.45
Al^{IV}			0.67	0.50	0.57	0.38	0.55
Al^{VI}			1.74	1.51	1.74	1.74	1.83
Ti			0.03	0.11	0.01	0.01	0.01
Fe			0.15	0.15	0.11	0.09	0.07
Mg			0.09	0.19	0.11	0.10	0.06
TOC			2.01	1.96	1.97	1.94	1.97
OC			−0.03	−0.22	−0.19	−0.27	−0.14
Ca			0.01	0.02	0.01	0.02	0.01
Na			0.09	0.08	0.01	0.01	0.02
K			0.47	0.44	0.68	0.56	0.64
P			0.02	0.03	0.00	0.00	0.00
ILC			0.68	0.71	0.71	0.61	0.68
LC			−0.70	−0.72	−0.76	−0.65	−0.69

ΣFe_2O_3: Total iron, LOI: Loss on ignition, TOC: Total octahedral cation, OC: Octahedral charge, ILC: Interlayer charge, LC: Layer charge.

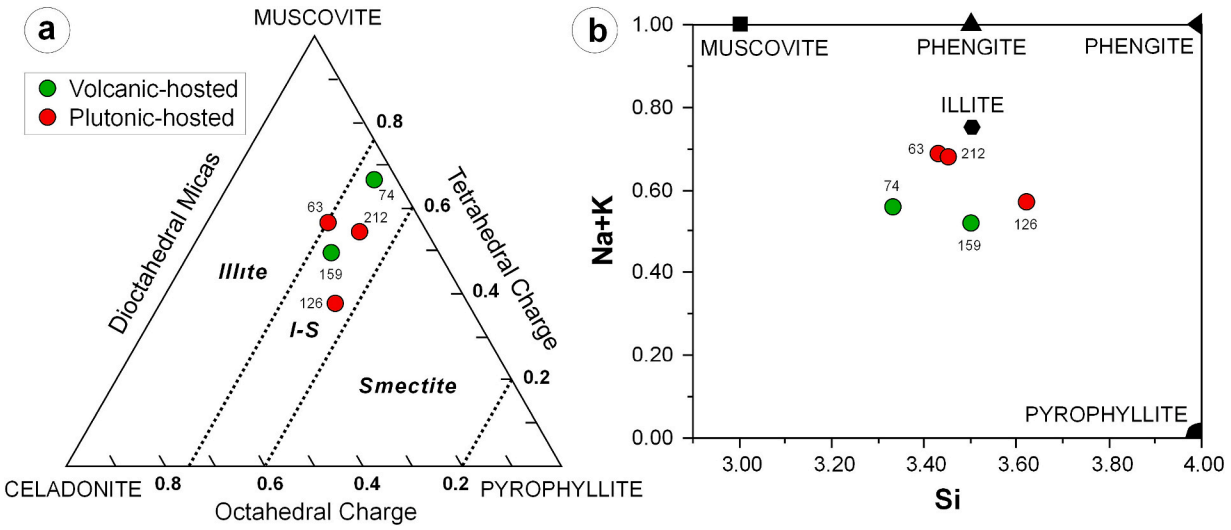

Fig. 7. Plot of structural data for illite (63, 126 and 212) and I—S (74 and 159) minerals in Tetrahedral charge vs. octahedral charge variation diagram (a) and Na + K vs. Si variation diagram (b).

light *REE* (L*REE*) concentrations are depleted with respect to high REE (H*REE*). All of the host-rocks and hydrothermal clays exhibit clear enrichment with respect to the chondrite.

Volcanic-hosted clays have 12–240 times enrichment compared to chondrite, whereas plutonic-hosted clays present relatively lower (5–100 times) enrichment than volcanic-hosted clays, hence they are clearly distinguished from each other. Normalized *REE* patterns of clays according to their volcanic- and plutonic-host rock compositions are given in Fig. 10b. Volcanic-hosted clays are rather close to their host rock composition, while plutonic plutonic-hosted clays have distinctly lower *REE* contents compared to their host rock composition. Plutonic-hosted clays exhibit considerably negative Eu anomaly, indicating that clays are derived from feldspars (K-feldspar). The chondrite-normalized Eu/Eu* (Sun and McDonough, 1989; Taylor and McLennan, 1985) and La_N/Lu_N ratios vs. K_2O contents of clay minerals exhibit notable relationships between *REE* and types of host-rocks (Fig. 11).

4.5.3. Oxygen and hydrogen isotopes

Stable-isotope compositions of hydrothermal clays are given in Table 4. Volcanic-hosted clays (R1 + R3 I—S) showed that the $\delta^{18}O_{SMOW}$ and δD_{SMOW} values vary from 12.9 to 13.5 ‰ and − 69 to −78 ‰, respectively. Plutonic-hosted clays (illite and R3 I—S) displayed relatively lower $\delta^{18}O_{SMOW}$ (8.2 to 10.2 ‰) but slightly higher δD_{SMOW} (−65 to −76 ‰) values than those of volcanic-hosted clays. The $\delta^{18}O_{SMOW}$ and δD_{SMOW} ranges of the clay minerals are given in Fig. 11, together with the lines of meteoric water (Craig, 1961) and supergene–hypogene

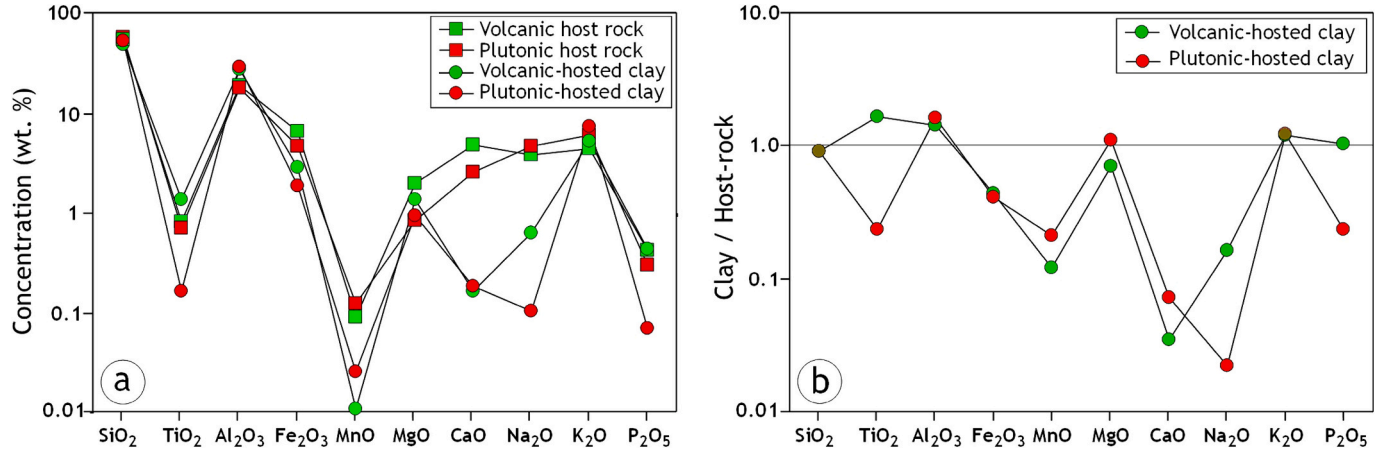

Fig. 8. a) Distributions of major element oxide concentrations of host-rocks and alteration related clay minerals, b) Host-rock normalized major element oxide values of alteration related clay minerals.

(Sheppard et al., 1969). The isotopic compositions of sea water, Eastern Mediterranean Meteoric Water (EMMW, $\delta^{18}O_{SMOW} = -6.12$ ‰, $\delta D_{SMOW} = -37.96$ ‰, Gat et al., 1996), and magmatic water ($\delta^{18}O_{SMOW} = 5.5$ to 9.5 ‰, $\delta D_{SMOW} = -40$ to -80 ‰, Taylor Jr, 1979) have also been given in the diagram.

Both plutonic- and volcanic-hosted clays represent typical hypogene conditions at relatively high temperatures, implying a more direct association with the hydrothermal fluids (Fig. 11a-b). The isotopic compositions of volcanic-hosted clays fall close to the supergene-hypogene line. The calculated isotopic ratios of fluids in equilibrium with clays were calculated from the clay-water fractionation factors (Savin and Lee, 1988 for $\delta^{18}O$ and Yeh, 1980 for δD) and show that clay-forming fluids evolve toward more positive $\delta^{18}O$ and more negative δD values with increasing temperature (Fig. 11a-b). The calculated equilibrium fluid composition corresponds to the average homogenization temperatures (~275 °C for plutonic-hosted phyllic zone, ~150 °C for volcanic-hosted argillic zone) from the primary fluid inclusions in quartz supporting a dominantly magmatic fluid origin (Fig. 11a-b). When the clay-forming fluids are assumed to be derived mainly from the magmatic water, the temperature conditions of plutonic-hosted clays are approximately 100 °C higher than volcanic-hosted clays, representing cooling of magmatic waters trend toward volcanic-hosted clays (Fig. 11c).

4.5.4. K—Ar dating

The age of plutonic-host rocks (Kösedağ Pluton) were previously determined by Kalkancı (1974, 1978) and Eyuboglu et al. (2017). The Rb—Sr whole-rock isochron age of quartz-syenite and pegmatitic biotite-syenite samples were determined as 42 ± 4 Ma and 37 ± 2.6 Ma (Kalkancı, 1974, 1978). The zircon U—Pb ages of four samples ranged from 44.6 ± 0.3 Ma to 42.3 ± 0.3 (Eyuboglu et al., 2017).

The first alteration age data, 38.0 ± 0.9 Ma, was presented by Başıbüyük (2006) from the K/Ar dating of alunite sample in the volcanic-hosted argillic zone. In addition to this, K—Ar dating was performed on two clay samples (I—S and illite) representing volcanic-hosted argillic and plutonic-hosted phyllic alterations in this study (Table 5). The age of the plutonic-hosted illite from phyllic zone (40.45 ± 1.28 Ma) is ~5 Ma older than the volcanic-hosted I—S from argillic zone (35.27 ± 2.81 Ma).

5. Discussion

5.1. Mineralogical evidences on the formation and origin of hydrothermal minerals

The formation of the hydrothermal minerals associated to sericitic (phyllic) and argillic alteration zones within the Karataş Volcanics and Kösedağ Pluton, in terms of mineralogical-petrographical perspective, was previously discussed (Başıbüyük and Yalçın, 2019). The argillic alteration zones which developed in the Karataş Volcanics are mainly characterized by clay/phyllosilicate minerals of kaolinite, pyrophyllite, R1 and R3 types of I—S accompanied by quartz, alunite, goyazite and jarosite minerals. The presence of pyrophyllite mineral, albeit in a small number of samples, indicates advanced argillic conditions in which temperatures exceeded 200 °C. However, pyrophyllite is stable at 275–350 °C in the Al_2O_3-SiO_2-H_2O system (Evans and Guggenheim, 1988), silica-saturated fluids can lead to the formation of pyrophyllite instead of kaolinite during hydrothermal alteration of silicates at low temperatures below 200 °C (Hemley et al., 1980; Berman, 1988).

The phyllic alteration zones developed within the Kösedağ Pluton are characterized by illite rich I—S (R3 type of I—S) and illite indicating the replacement on the K-feldspars as well as direct precipitation from hydrothermal solutions with high K^+ activity (log $(a_K^+/a_H^+ > 2$, according to K_2O-Al_2O_3-SiO_2-H_2O system at quartz saturation: Sverjensky et al., 1991; Inoue, 1995) at temperature conditions >200 °C.

According to optical microscopic data, I—S minerals formed in the volcanic matrix in the volcanic-hosted argillic zones, whereas I—S and illites occurred as replacement feldspar minerals in the plutonic-hosted phyllic zones as formulized below:

Volcanic glass → Hydrous Al-silica gel → I—S

$$6SiO_2{\cdot}3Al_2O_3{\cdot}Na_2O{\cdot}K_2O + 19H_2O + 4H^+ \rightarrow 6Al(OH)_3 \cdot 6Si(OH)_4 \rightarrow KNaAl_4[Al_2Si_6O_{20}](OH)_4 + 18OH^-$$

Orthoclase → I—S or illite/muscovite

$$6KAlSi_3O_8 + Na^+ + 4H_2O \rightarrow 2(K,Na)_{0.5}Al_2[AlSi_3O_{10}](OH)_2 + 12SiO_2 + 5\,K^+ + 4OH^-$$

$$4KAlSi_3O_8 + 6H^+ \rightarrow KAl_3(Si_3AlO_{10})(OH)_2 + 9SiO_2 + 2H_2O + 3\,K^+$$

(Plagioclase → I—S)

$$3(Na,Ca)Al_2Si_2O_8 + 2H_2O + K^+ + 2H^+ \rightarrow 2(K,Na)_{0.5}Al_2[AlSi_3O_{10}](OH)_2 + 2\left(Na^+, Ca^{2+}\right) + 2OH^-$$

The presence of illite and I—S describes the changes of the hydrothermal conditions from highly acidic to neutral conditions. Ordering types and/or illite percentages in I—S are mainly related to temperature conditions in sedimentary-diagenetic and hydrothermal environments (Frey, 1987; Inoue, 1995, 2005; Merriman and Peacor, 1999; Ylagan et al., 2000). In terms of I—S formations in sedimentary and hydrothermal environments; Bethke et al. (1986) pointed out the formation of l-S minerals in hydrothermal systems is a simple result of direct

Table 3
Trace element and *REE* (ppm) compositions of magmatic host rocks and clay minerals (n = number of samples).

Sample	Karataş volcanics	Kösedağ Q-Syenite	I-S (Volcanic-hosted)		Illite (Plutonic-hosted)		
	Average (n = 4)	ZK-56	ZK-74	ZK-159	ZK-63	ZK-126	ZK-212
Cr	20	<20	62	<20	<20	<20	<20
Ni	<20	<20	<20	<20	<20	<20	<20
Co	16	8	25	2	12	4	3
Sc	20	8	29	42	7	4	5
V	179	94	413	308	89	115	38
Cu	48	55	98	91	46	14	<10
Pb	19	23	8	25	265	54	<5
Zn	108	59	<30	136	596	31	75
Bi	0.1	<0.1	<0.1	0.2	0.2	0.2	<0.1
In	0.1	<0.1	<0.1	<0.1	<0.1	<0.1	<0.1
Sn	2	6	6	1	2	2	2
W	34.3	49.4	70.1	14.9	265	114	67.6
Mo	2	<2	<2	4	2	7	2
As	12	14	67	30	28	1130	40
Sb	3	2.5	0.5	5.0	23.3	49.2	19.0
Ge	1.8	1.3	1.4	2.3	0.6	0.6	0.8
Be	3	3	3	4	5	3	5
Ag	0.7	<0.5	<0.5	1.9	3.8	5.0	0.5
Rb	147	202	127	188	487	318	308
Cs	7.4	6.2	33.5	30.6	38.1	34.8	12.8
Ba	805	1100	379	585	69	1080	6
Sr	599	515	507	976	20	45	49
Tl	0.39	0.77	2.70	2.10	2.74	16.90	0.71
Ga	21	18	30	32	36	34	38
Ta	0.91	0.70	0.70	1.43	1.88	0.96	0.71
Nb	15.3	10.7	7.3	22.9	5.9	6.9	6.5
Hf	5.5	2.8	5.0	7.7	2.5	4.4	2.2
Zr	206	95	171	254	78	185	78
Y	27.1	18.4	18.6	39.9	11.3	13.8	13.4
Th	11.43	7.84	7.36	15.10	10.20	10.30	14.90
U	3.77	1.94	2.62	4.77	5.43	5.51	2.06
La	32.43	28.60	16.90	56.30	24.60	11.10	18.90
Ce	57.9	53.6	32.7	109.0	45.4	19.9	36.5
Pr	6.28	6.20	3.90	11.50	4.39	1.91	3.66
Nd	27.0	23.7	15.5	49.8	16.9	7.8	14.9
Sm	5.95	4.76	3.10	6.82	3.18	1.65	2.76
Eu	1.550	1.330	0.749	1.550	0.488	0.411	0.288
Gd	5.15	3.91	2.45	4.78	2.19	1.53	1.85
Tb	0.82	0.63	0.46	0.74	0.30	0.29	0.31
Dy	4.53	3.60	3.26	5.48	1.71	1.89	2.03
Ho	0.86	0.73	0.70	1.27	0.34	0.42	0.43
Er	2.79	2.25	2.26	4.56	1.13	1.44	1.42
Tm	0.420	0.343	0.349	0.749	0.184	0.235	0.226
Yb	2.54	2.19	2.11	4.51	1.14	1.50	1.42
Lu	0.400	0.323	0.315	0.731	0.179	0.253	0.219
REE_{tot}	148.62	132.17	84.75	257.79	102.13	50.33	84.91
La_N/Lu_N	8.69	9.49	5.75	8.25	14.73	4.70	9.25
Eu/Eu*	0.86	0.94	0.83	0.83	0.57	0.79	0.39

REE_{tot} = Total REE, $Eu/Eu^* = Eu_N/(Sm_N \cdot Gd_N)^{0.5}$.

precipitation from solution, controlled by the ambient temperature, pressure, and solution composition at arbitrary conditions. They questioned the direct application of the diagenetic reaction series of smectite to illite transformation to the series found in hydrothermal systems. In contrary, Inoue et al. (1992) indicated that the formation of I-S minerals in hydrothermal systems is basically identical to that which occurs in diagenetic environments, i.e., that it is due to a consecutive reaction from an early-formed smectite to illite through I-S. Field observations, textural and mineralogical data obtained from this study are compatible with the approach of direct precipitation of I—S and illite from solution which was principally controlled by the ambient temperature and composition of hydrothermal fluids (Bethke et al., 1986; Murakami et al., 2005), rather from previously-formed smectite transforming to illite via I—S (Inoue et al., 1992). The observation of hydrothermal I—S and illites as single mineral phases, as seen in our study, were reported as related to pervasive alteration (Eberl et al., 1987; Ylagan et al., 2000).

The acicular/fibrous morphology of I—S under SEM are similar to those of ordered I—S or illite exhibiting acicular or lath forms (Nadeau et al., 1984a, 1984b; Inoue et al., 1987; Inoue and Kitagawa, 1994; Inoue, 1995). The laths of I—S and illites, elongating to the *a*-axis direction, are also characteristic for 1 *M* polytype in hydrothermal environments (e.g., Inoue et al., 1992; Inoue and Kitagawa, 1994). The presence of 1 *M* polytype accompanies 1 M_d polytype, albeit in small amounts, in R3 I—S (90 % I in I—S) and illites seems to be related to magmatic (volcanic-pyroclastic) origin as previously stated in several studies (e.g., Zviagina et al., 2015; Bozkaya et al., 2016, 2019b, 2021).

Particle thickness or crystallite size of I—S increases with decreasing smectite % contents. The swelling (smectite) layer percent (3–5 %) and crystallite sizes (*N* = 15–20 nm) of two illites (ZK-63 and ZK-212) are similar to those of hydrothermal illites (e.g., Środoń et al., 1992). The temperature conditions of hydrothermal I—S and illites have been suggested as higher than 200 °C (phyllic alteration) for illite or low smectite content I—S (R3 type of I—S), and below 200 °C for intermediate I—S (R1 type of I—S) (Velde, 1985; Ylagan et al., 2000; Parry et al., 2002; Inoue, 2005).

According to the above data, relatively higher temperature

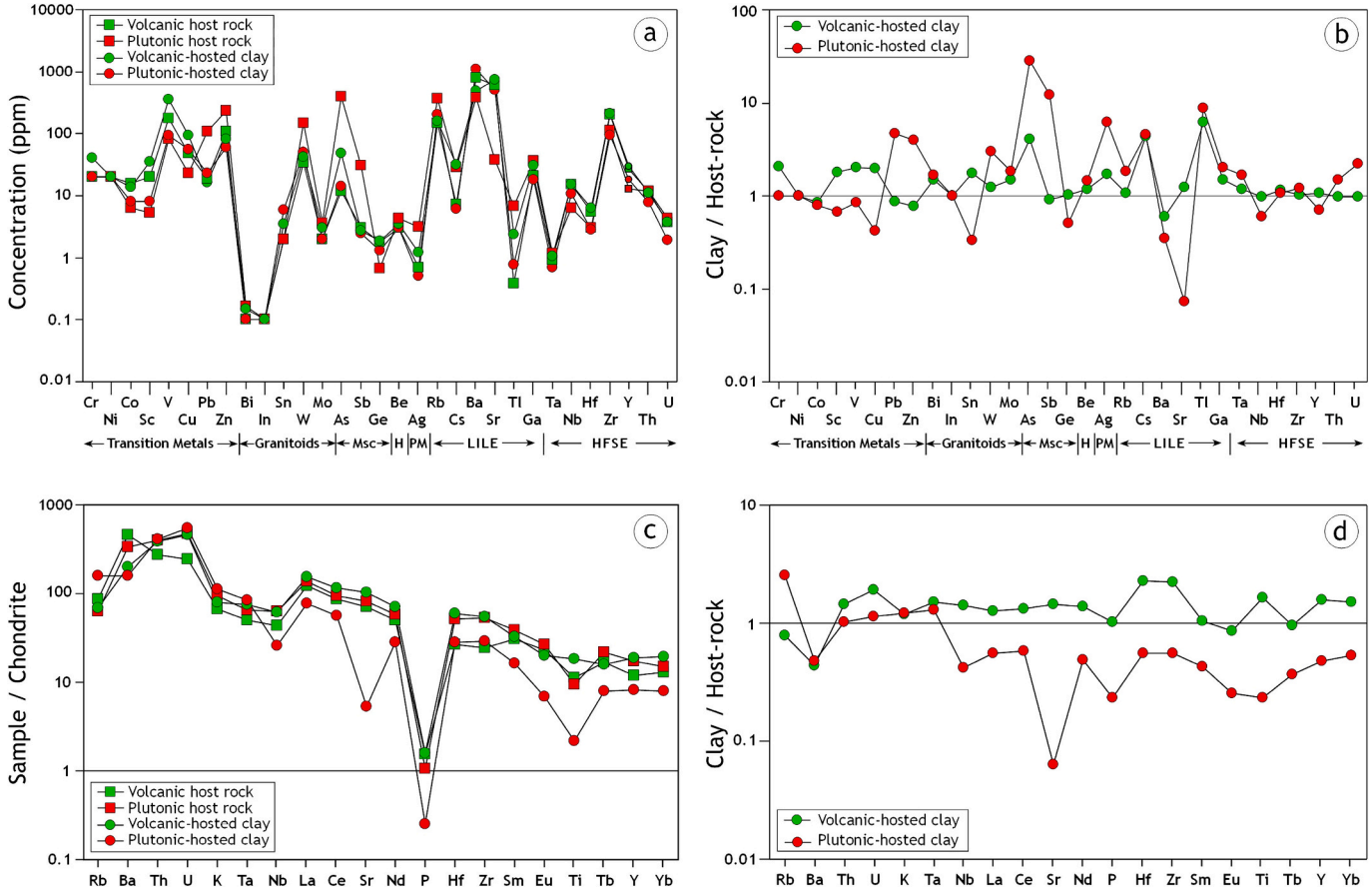

Fig. 9. a) Distributions of trace element concentrations of host-rocks and alteration related clay minerals, b) Host-rock normalized trace element values of alteration related clay minerals, c) Chondrite-normalized distributions of some major oxides, trace elements and *REE* of host-rocks and alteration related clay minerals, e) Host-rocks normalized distributions of some major oxides, trace elements and *REE* of alteration related clay minerals.

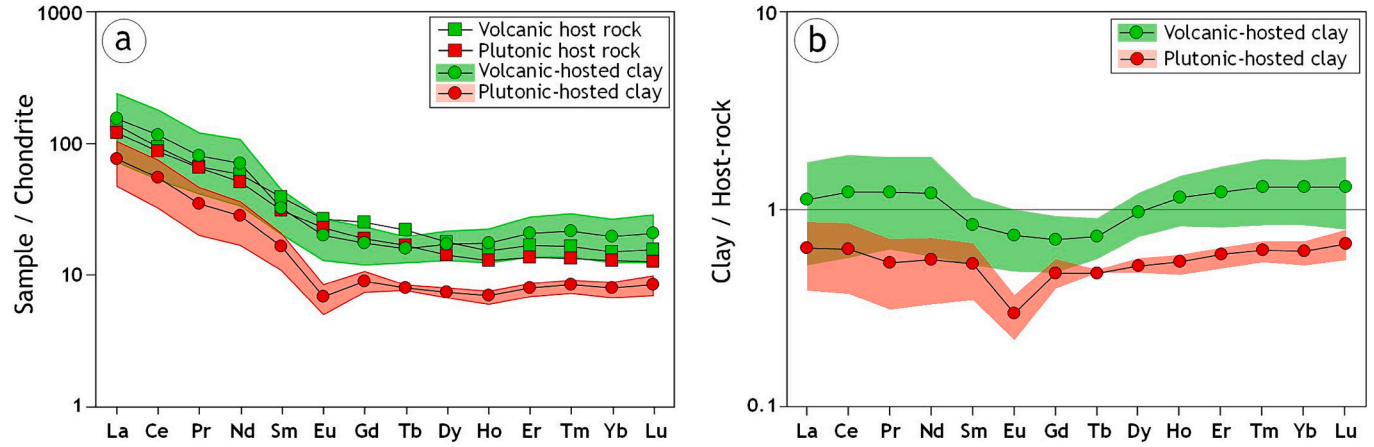

Fig. 10. a) Chondrite-normalized *REE* patterns of host-rocks and alteration related clay minerals, b) Host-rocks normalized distributions *REE* patterns of alteration related clay minerals.

conditions and higher K^+ ion activities (a_K^+) of hydrothermal fluids caused the illites and R3 type I—S in the plutonic-hosted phyllic alteration zones. However, relatively low temperature conditions and low K^+ ion activities (a_K^+) caused the formation of R1 type I—S in the volcanic-hosted argillic alteration zones.

5.2. Geochemical evidences on the formation and origin of hydrothermal minerals

The smectite illitization in hydrothermal systems is generally completed during a short period of time (probably within one million years), although there are a few exceptions, as determined by K—Ar dating of I-S minerals (Inoue et al., 1992). This time scale is almost equivalent to the life-time of a single hydrothermal event (Wohletz and

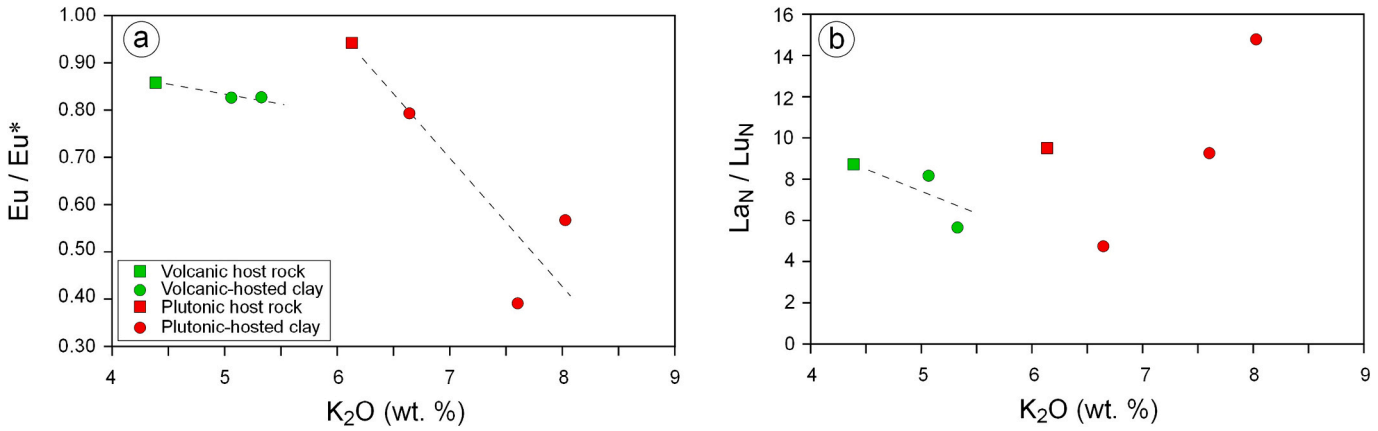

Fig. 11. Plots of some elemental ratios and K_2O for host-rocks and clay minerals (a) Eu/Eu* vs. K_2O, (b) La_N/Lu_N vs. K_2O.

Table 4
Stable isotopic (O, H) compositions (‰) of clay minerals.

Sample	Host-rock	Mineral	Type	δD (SMOW)	$\delta^{18}O$ (SMOW)
ZK-74	Volcanic	I-S	R3 + R1	−69	12.9
ZK-159		I-S	R3 + R1	−78	13.5
ZK-63	Plutonic	Illite	–	−68	8.2
ZK-126		I-S	R3	−76	11.2
ZK-212		Illite	–	−65	10.2

Table 5
K—Ar dating of volcanic hosted I—S and plutonic-hosted illite samples.

Sample	% K_2O	Mass [mg]	% K	% 40Ar*	Age avg. [Ma]	Error avg. [Ma]
ZK-74	5.465	11.06	4.536	23.5	35.68	5.58
(I—S)				42.2	34.87	2.37
Volcanic				Average	35.27	2.81
ZK-63 (Ilt)	8.627	28.64	7.161	66.9	40.45	1.28
Plutonic						

Heiken, 1992). K—Ar dating of micaceous materials including l-S and illite is beneficial in allowing one to distinguish each stage of the different hydrothermal alterations superimposed at a site (Sawai et al., 1989; Wolde-Gabriel and Goff, 1989, 1992; Inoue and Utada, 1991).

The chemical composition of l-S changes continuously from one end point of a montmorillonite smectite to another end point of illite, but the path line is different for various geologic origins because the precursor smectites have different layer charges (Velde and Brusewitz, 1986; Meunier and Velde, 1989).

The layer charges of investigated illite and I—S are about 0.70–0.75/(O_{10}) $(OH)_2$ lower than those of typical illite layer charge (0.90/(O_{10}) $(OH)_2$) in the literature (Meunier and Velde, 1989; Środoń et al., 1992). The interlayer K increases whereas octahedral Fe and Mg decrease with increasing % illite as reported for both diagenetic and hydrothermal environments (Inoue, 1995).

The several geochemical parameters (pH, salinity and/or alkalinity, silica saturation, water and ion activity, degree of leaching in open or close systems and composition of host-rocks) should control the type of clay minerals in the study area, such as kaolinite and I—S in volcanic-hosted argillic alteration zone, while I—S and illite in plutonic-hosted phyllic alteration zone (Bohor and Triplehorn, 1993; Gündoğdu et al., 1996; Ece et al., 2003). Volcanic-hosted argillic alteration zones are characterized by environmental conditions such as lower pH (acid to neutral), alkalinity, K+ activity (aK+) and higher silica saturation, leaching degree and water activity than plutonic-hosted phyllic alteration zones.

The major, trace and *REE* compositions of host-rocks and hydrothermal clays and normalized patterns according to chondrite and host-rocks indicate that the formations of hydrothermal clays were principally influenced by the composition of host-rocks (See Figs. 7 to 10). Although the concentrations of rare earth elements (*REE*) are more enriched in the volcanic-hosted I—S in comparison with the plutonic-hosted I—S and illites indicating illitic minerals are derived from volcanic glass in volcanic host-rocks and from K-feldspar in plutonic host-rocks. The variations in trace-element and, in particular, *REE* distributions in the I—S and illites reflect also change in diagenetic grade or increasing temperature, as established by some researchers (e.g. Awwiller and Mack, 1991; Milodowski and Zalasiewicz, 1991; Ohr et al., 1994; Bozkaya and Yalçın, 2010). In this context, different mineralogical and geochemical characteristics of hydrothermal clays are associated to different formation conditions, i.e. temperature, fluid composition, pH, alkalinity etc., in other words, they are related to plutonic- and volcanic-hosted rocks having different conditions.

La_N/Yb_N and Eu/Eu* ratios were employed to demonstrate the REE fractionation (Fig. 11). The increase of Eu/Eu* ratios of clays, but decrease of La_N/Yb_N ratios in plutonic-hosted clays from phyllic alteration are characteristic tool for magmatic-hydrothermal systems (Shikazono et al., 2008; Parsapoor et al., 2009).

The negative Eu anomaly increases with increasing K_2O or illite contents in I—S (Bozkaya and Yalçın, 2010). The Eu anomaly generally reflects a specific origin, mobility, or fractionation (e.g., Uysal and Golding, 2003; Honty et al., 2008). Increasing Eu anomalies from volcanic-hosted R1 + R3 I—S to plutonic-hosted R3 I—S and illites may be explained by volcanogenic feldspar, considered to be a reference-mineral phase controlling Eu mobility.

The distinctive Eu anomaly should be derived by alteration of feldspars. La_N/Lu_N ratios of I—S and illite, reflecting H*REE* enrichment relative to L*REE*, have an almost regular distribution; increasing from plutonic-hosted R3 I—S and illite to volcanic-hosted R1 + R3 I—S in relation to their K_2O contents, thus indicating the positive relation between La_N or L*REE* and illite interlayers. Only L*REE* can fit in the illite interlayers, and thus the I—S interlayer sites should preferentially accumulate L*REE*s relative to H*REE*s during progressive illitization if I—S mineralization controls *REE* fractionation (Awwiller, 1994).

According to fluid inclusion homogenization temperature data obtained from plutonic and volcanically hosted hydrothermal quartz, isotope fractions of I—S and illites provided clear evidence of the magmatic origin of hydrothermal fluids (see Fig. 12). The temperature conditions obtained from isotope and fluid inclusion data are compatible to crystal-chemical data of I—S and illites, with almost 75–100 °C difference between plutonic-hosted (phyllic) and volcanic-hosted (argillic) clay occurrences.

The wide range in hydrogen- and oxygen-isotopic values indicate that hydrogen-isotope values were not changed and rearranged during

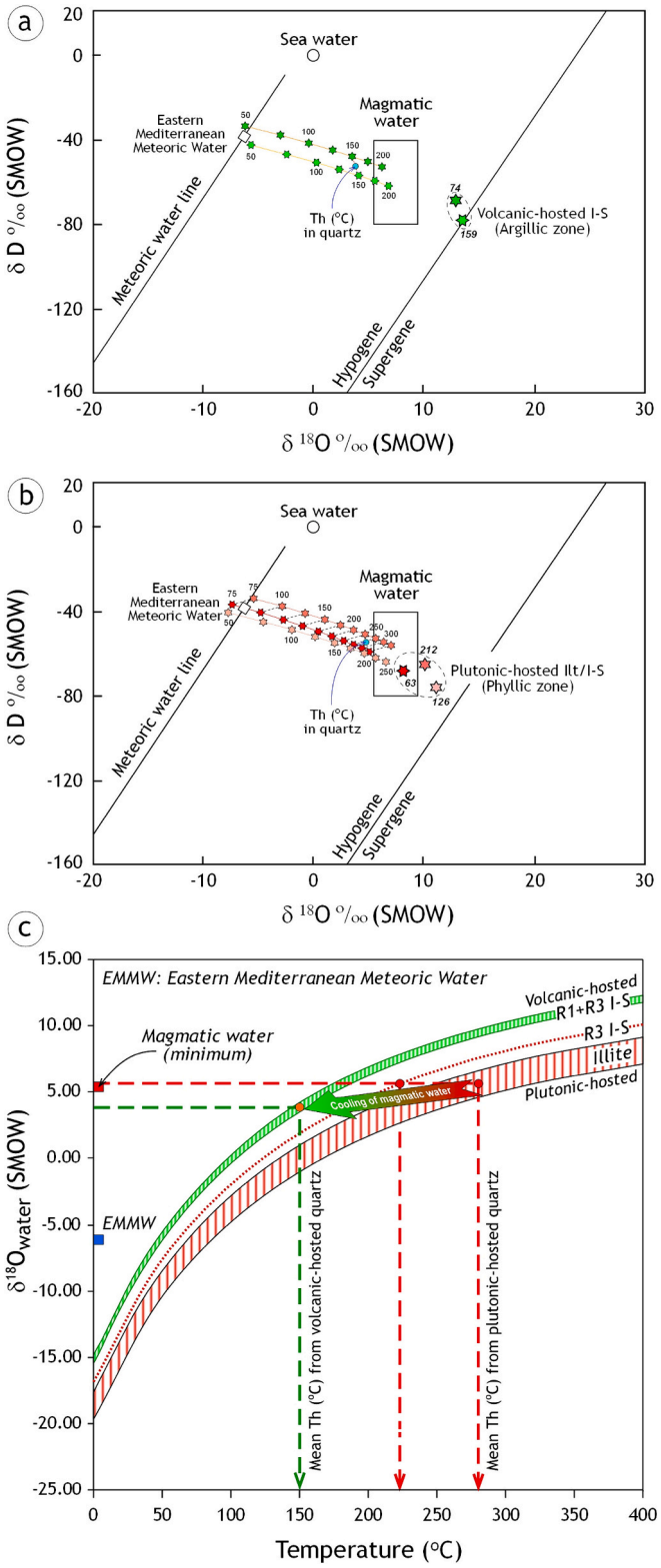

Fig. 12. Plots of δD vs. $\delta^{18}O$ values of (a) volcanic- and (b) plutonic-hosted illite and I—S minerals and distributions of their mineral-water equilibria. c) Calculated oxygen isotopic values of waters in equilibrium with clays showing the decreasing temperatures (cooling of waters) from plutonic to volcanic host-rocks. The average homogenization temperatures (Th, °C) from the plutonic- and volcanic-hosted quartz were also given for comparison.

post-hydrothermal processes, as mentioned by Longstaffe and Ayalon (1990). The observation of regular isotopic distribution together with increasing temperature indicate some differences of the mineral-forming fluids for plutonic- and volcanic-hosted hydrothermal clays associated with fluid-rock interactions (Bechtel et al., 1999) for different host rocks. Clay mineral-forming fluids with magmatic water origin are approximately 100 °C higher in plutonic-hosted phyllic zones than volcanic-hosted argillic zones, and represent cooling of magmatic waters from plutonic- to volcanic-hosted alteration zones. These data clearly indicate that the hydrothermal fluids were originated from the Kösedağ Pluton, wherein temperature conditions were relatively higher than in volcanic-host rocks, and caused the development of successive phyllic and argillic alterations in plutonic and volcanic host-rocks, respectively.

5.3. Hydrothermal alteration model

The first volcanic activity was observed as pyroclastic layers within the Middle-Upper Eocene Akıncılar Formation which passes to the Karataş Volcanics with an agglomeratic level. The volcanic activity started from Middle Eocene in the region and continued until the end of Eocene in the form of lava flows. Before Karataş Volcanics have yet not completely cooled, the syenites have settled by ascending up to shallow depths with hot-hot contact (Başıbüyük, 2006). The fracture or cracks zones were developed related to increasing pressure of the volatile components in the pluton, after the solidification of plutonic and volcanic rocks and enabled the circulation of hydrothermal solutions of magmatic origin and caused changes in both plutonic and volcanic rocks (Fig. 13). Two main alteration systems have been effective. The first one involves later stage processes and deuteric hydrothermal fluids which effective within the top of a large volume of the Kösedağ pluton, namely plutonic-hosted propylitic and phyllic alterations. Other one is a fracture-controlled hydrothermally altered zone at the margins of the Kösedağ pluton within the volcanics, namely volcanic-hosted argillic alteration. The distribution of propylitic alteration zones is very small and developed only in a few-meter zone within the volcanics at the plutonic-volcanic contact (Fig. 13). The argillic alteration zones widely affected volcanic rocks, because of the extensive circulating of hydrothermal fluids were developed within the volcanic rocks, which probably resulted from relatively fast fluid-rock interactions (dissolution-precipitation) with fine-grained components (volcanic glass and microlites in the matrix) relative to syenites. Başıbüyük (2006) stated that hydrothermal alterations are concentrated in the volcanics surrounding the plutonic body as well as two main tectonic zones developed along the NE-SW direction.

As confirmed by K—Ar dating of alunite, I—S and illite minerals (Fig. 14); the hydrothermal alteration was started at 40.45 ± 1.28 Ma (Bartonian) within the plutonic body as phyllic alteration stage, almost 2 Ma after the youngest age of Q-syenite (42.3 ± 0.3 Ma, Eyuboglu et al., 2017). Hydrothermal alteration was continued as argillic alteration stage according to ages of alunite (38.0 ± 0.9 Ma, Başıbüyük, 2006) and I—S (35.27 ± 2.81 Ma) with a duration of ~5 Ma. The age data show that hydrothermal alteration ended before the exhumation of the Kösedağ Pluton (28–30 Ma, Boztuğ and Jonckheere, 2007) and that it formed in association with a typical magmatic-hydrothermal system. The age ranges for pegmatitic syenite and alteration minerals indicate late stage processes as alteration and mineralization associated with syenitic intrusion. In addition to phyllic and argillic alterations, scarce propylitic alteration zones and Fe-Pb-Zn deposits were also developed in the study area (Efe and Gökçe, 1999; Başıbüyük, 2006).

6. Conclusions

The propylitic and phyllic alteration in the plutonic rocks and argillic alteration in the volcanic rocks were developed as a result of intrusion of the Kösedağ Pluton into Karataş Volcanics with relations of hot-hot contact. The hydrothermal alteration related minerals are represented

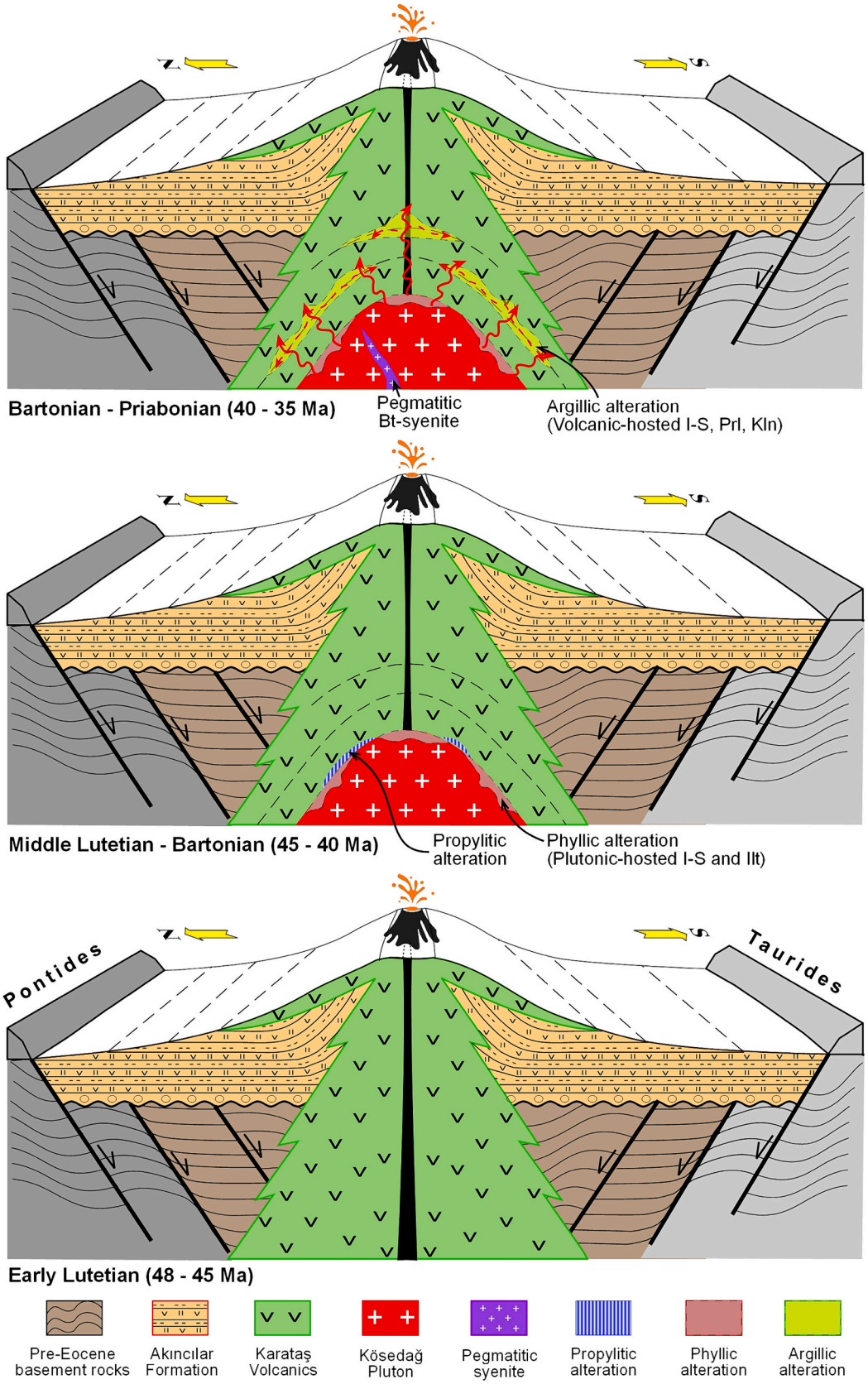

Fig. 13. The schematic model for the origin of clay mineral-forming hydrothermal fluids in which temperature conditions decrease from plutonic-hosted alteration zones to volcanic-hosted alteration zones.

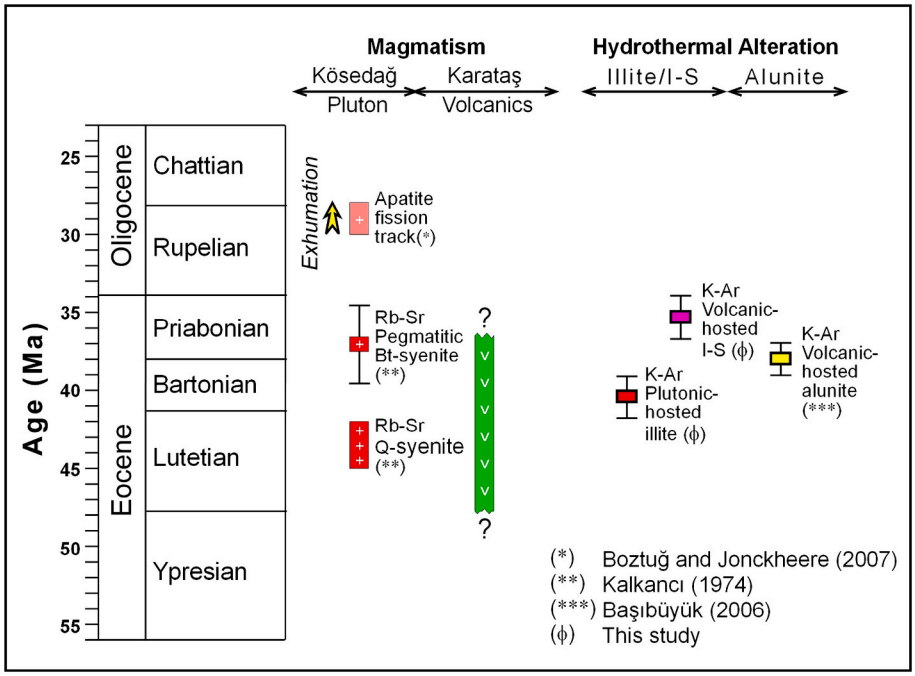

Fig. 14. Distribution of age data for magmatism and hydrothermal alterations, indicating the cooling trend from phyllic to argillic alteration with duration of 5 Ma, before the exhumation of Kösedağ Pluton.

by phyllosilicate/clay, iron oxide and hydroxide (hematite, goethite), carbonate (calcite and dolomite), sulfate (barite, alunite and jarosite), phosphate (goyazite), silica (quartz and opal-CT) and other silicate (epidote) minerals. Phyllosilicate/clay minerals are kaolinite, illite, smectite, chlorite, mixed layers I—S and C—S, pyrophyllite. The ordering types of I—S are R1 I—S (I = 65–80 % in I—S) and R3 I—S (I = 90 % in I—S) in the volcanic-hosted rocks, and R3 I—S (I = 90 % in I—S) in the plutonic-hosted rocks. The polytypes of illite and R3 I—S are determined as 1 $M_d \pm 1\ M \pm 2\ M_1$ and 1 $M_d + 1\ M$, respectively. $d_{(060)}$ values of R1 and R3 I—S and illites range from 1.494 to 1.500 Å and represent dioctahedral composition. I—S and illites are derived from feldspar in the plutonic host-rocks, but both from feldspar and volcanic glass in the volcanic host-rocks during hydrothermal alteration.

The average homogenization temperatures of fluid inclusions trapped in hydrothermal quartz crystals associated to clays were measured as 275 °C and 150 °C a for primary inclusions in plutonic- and volcanic-hosted quartz, respectively. Plutonic-hosted quartz crystals show relatively higher temperature and salinity values than those of volcanic-hosted ones, similarly to mineralogical data of clay minerals.

The differences in the major oxide compositions of volcanic- and plutonic-hosted illitic clays appear to be associated to their host rock compositions, based on the similarity of the SiO_2, Al_2O_3 and K_2O contents of I—S to the host rock. Trace element compositions of I—S and illites differ from those of host-rocks, and they are enriched in the volcanic-hosted clays, but depleted in the plutonic-hosted clays. *REE* concentrations of clays compared to host-rocks show that volcanic-hosted clays are similar to volcanic host-rocks, whereas there is a distinct depletion for plutonic-hosted clays as well as Eu negative anomaly, indicating they derived from K-feldspars. Oxygen and hydrogen isotopic compositions of volcanic- and plutonic-hosted clays indicate the hypogene conditions of formation associated to hydrothermal fluids originated from magmatic waters and display some differences with respect to their host-rocks. When the stable isotope data and fluid inclusion data were evaluated together, it has been determined that the plutonic-hosted clays have been formed at temperature conditions higher than ~100 °C.

K—Ar data of alunite, I—S and illite minerals point out approximately 5 Ma duration for hydrothermal alteration which started at 40.45 ± 1.28 Ma for illite as phyllic stage, via 38.0 ± 0.9 Ma for alunite and ended at 35.27 ± 2.81 Ma for I—S as argillic stage. The hydrothermal alteration was developed almost 2 Ma after the intrusion of Kösadağ Pluton, and ended before the exhumation of the Kösedağ Pluton (28–30 Ma).

As a conclusion, the mineralogical and geochemical data from illitic clay minerals may play a critical role for understanding origin, age (or duration) and conditions of the hydrothermal alterations.

CRediT authorship contribution statement

Ömer Bozkaya: Writing – original draft, Methodology, Investigation, Conceptualization. **Zeynel Başıbüyük:** Methodology, Investigation, Conceptualization. **Hüseyin Yalçın:** Methodology, Investigation, Conceptualization. **Gülcan Bozkaya:** Methodology, Investigation, Data curation. **Deniz Hozatlıoğlu:** Methodology, Investigation, Data curation. **Marek Szczerba:** Methodology, Data curation.

Declaration of competing interest

The authors declare that they have no known competing financial interests or personal relationships that could have appeared to influence the work reported in this paper.

Acknowledgements

This research was funded by Sivas Cumhuriyet University Scientific Research Project Office (Project Number: M-215). Marek Szczerba acknowledges financial support from the NCN: OPUS 2020/37/B/ST10/01697 for K-Ar dating. The authors thank to Editor-in-Chief Dr. Astrid Holzheid and Guest Editor Dr. Emin Çiftçi for editorial handling, and three anonymous referees for their valuable contributions to the improvement of the manuscript for their constructive suggestions.

References

Awwiller, D.N., 1994. Geochronology and mass transfer in Gulf Coast mudrocks (south-central Texas, U.S.A.): Rb-Sr, Sm-Nd and *REE* systematics. Chem. Geol. 116, 61–84.

Awwiller, D.N., Mack, L.F., 1991. Diagenetic modifications of Sm-Nd model ages in Tertiary sandstones and shales, Texas Gulf Coast. Geology 19, 311–314.
Başıbüyük, Z., 2006. Hydrothermal Alteration Mineralogy- Petrography and Geochemistry of Eocene Volcanics: An Example From Quadrangle of Zara-Imranli-Suşehri-Şerefiye (Northeast of Sivas, Central-Eastern Anatolia, Turkey). Sivas Cumhuriyet University, Graduate School of Natural and Applied Sciences (PhD Thesis, 269 p).
Başıbüyük, Z., Yalçın, H., 2019. Mineralogy, petrography and origin of hydrothermal alteration in Eocene magmatites in Central Anatolia (Sivas-Turkey). Bull. Min. Res. Exp. 158, 141–164.
Bechtel, A., Savin, S.M., Hoernes, S., 1999. Oxygen and hydrogen isotopic composition of clay minerals of the Bahloul formation in the region of the Bou Grine zinc-lead ore deposit (Tunisia): evidence for fluid-rock interaction in the vicinity of salt dome cap rock. Chem. Geol. 156, 191–207.
Berman, R.G., 1988. Internally-consistent thermodynamic data for minerals in the system Na_2O-K_2O-CaO-MgO-FeO-Fe_2O_3-Al_2O_3-SiO_2-TiO_2-H_2O-CO_2. J. Petrol. 29, 445–522.
Bethke, C.M., Vergo, N., Altaner, S.P., 1986. Pathways of smectite illitization. Clay Clay Miner. 34, 125–135.
Bingöl, E., 1989. 1/2.000.000 scaled geological map of Turkey. In: General Directorate of Mineral Exploration and Research (MTA), Ankara, Turkey.
Bohor, B.F., Triplehorn, D.M., 1993. Tonsteins: altered volcanic ash layers in coal bearing sequences. Geol. Soc. Am. Spec. Pap. 285 (44 pp).
Bozkaya, Ö., Yalçın, H., 2010. Geochemistry of mixed-layer illite-smectites from an extensional basin, Antalya Unit, Southwestern Turkey. Clay Clay Miner. 58, 644–666.
Bozkaya, Ö., Bozkaya, G., Uysal, I.T., Banks, D.A., 2016. Illite occurrences related to volcanic-hosted hydrothermal mineralization in the Biga Peninsula, NW Turkey: implications for the age and origin of fluids. Ore Geol. Rev. 76, 35–51.
Bozkaya, Ö., Bozkaya, G., Yılmaz, H., Hozatlıoğlu, D., Banks, D.A., 2019a. The origin, age and duration of hydrothermal alteration associated with iron skarn mineralization determined from clay/phyllosilicate minerals, Bizmişen-Erzincan, East-Central Turkey. Ore Geol. Rev. 115, 103179.
Bozkaya, Ö., Bozkaya, G., Hanilçi, N., Laçin, D., Banks, D.A., Uysal, İ.T., 2019b. Mineralogical and geochemical evidence of late epithermal alteration in the Kisladag porphyry gold deposit, Usak, Western Turkey. In: Life with Ore Deposits on Earth, 15th Biennial SGA Conference, 27–30 Aug 2019, Glasgow. Society for Geology Applied to Mineral Deposits, Proceedings, 3, pp. 1031–1034.
Bozkaya, Ö., Günal-Türkmenoğlu, A., Göncüoğlu, M.C., Okuyucu, C., 2021. Geological, mineralogical and geochemical characteristics of Mississippian K-bentonites from southern Turkey: a correlation with coeval tephras from Gondwana-derived terranes. J. Asian Earth Sci. 181, 104258.
Boztuğ, D., 2007. Petrogenesis of the Kösedağ Pluton, Suşehri-NE Sivas, East-Central Pontides, Turkey. Turk. J. Earth Sci. 17, 241–262.
Boztuğ, D., Jonckheere, R.C., 2007. Apatite fission track data from central Anatolian granitoids (Turkey): constraints on neo-Tethyan closure. Tectonics 26, TC3011.
Clayton, R.N., Mayeda, T.K., 1963. The use of bromine pentafluoride in the extraction of oxygen from oxides and silicates for isotopic analysis. Geochim. Cosmochim. Acta 27, 43–52.
Corbett, G.J., Leach, T.M., 1998. Southwest Pacifiic Rim gold-copper systems: structure, alteration, and mineralization. In: Society of Economic Geologists, Special Publication, No: 6, p. 237.
Craig, H., 1961. Isotopic variations in meteoric waters. Science 133, 1702–1703.
Dill, H., Bosse, H.-R., Henning, K.-H., Fricke, A., Ahrendt, H., 1997. Mineralogical and chemical variations in hypogene and supergene kaolin deposits in a mobile fold belt the Central Andes of northwestern Peru. Miner. Deposita 32, 149–163.
Dill, H., Bosse, H.-R., Kassbohm, J., 2000. Mineralogical and chemical ctudies of volcanic-related argillaceous industrial minerals of the Central American Cordillera (Western El Salvador). Econ. Geol. 95, 517–538.
Eberl, D.D., Velde, B., 1989. Beyond the Kübler index. Clay Miner. 24, 571–577.
Eberl, D.D., Srodon, J., Lee, M., Nadeau, P.H., Northrop, H.R., 1987. Sericite from the Siverton caldera, Colorado: correlation among structure, composition, origin and particle thickness. Am. Mineral. 72, 914–934.
Ece, Ö.I., Nakagawa, Z.E., Schroeder, P.A., 2003. Alteration of volcanic rocks and genesis of kaolinite deposits in the Şile region, northern İstanbul, Turkey. I: clay mineralogy. Clay Clay Miner. 51, 675–688.
Ece, Ö.I., Schroeder, P.A., Smilley, M., Wampler, M., 2008. Acid-sulfate alteration volcanic rocks and genesis of halloysite and alunite deposits in the Biga Peninsula, NW Turkey. Clay Miner. 43, 281–315.
Ece, Ö.İ., Ekinci, B., Schroeder, P.A., Crowe, D., Esenli, F., 2013. Origin of the Düvertepe kaolinite-alunite deposits in Simav Graben, Turkey: timing and styles of hydrothermal mineralization. J. Volcanol. Geotherm. Res. 255 (57-18).
Efe, A., Gökçe, A., 1999. Geology and fluid inclusion studies of Pb-Zn deposits around Maden village (İmranlı-Sivas). Cumhuriyet Univ. Bull. Fac. Eng. Ser. A Earth Sci. 16, 29–38.
Evans, B.W., Guggenheim, S., 1988. Talc, pyrophyllite, and related minerals. In: Bailey, S.W. (Ed.), Hydrous Phyllosilicates (Exclusive ofMicas), Reviews in Mineralogy 19. Mineralogical Society of America, Washington, D.C, pp. 225–294.
Eyuboglu, Y., Dudas, F.O., Thorkelson, D., Zhu, D.-C., Liu, Z., Chatterjee, N., Yi, K., Santosh, M., 2017. Eocene granitoids of northern Turkey: polybaric magmatism in an evolving arc–slab window system. Gondw. Res. 50, 311–345.
Ferreiro-Mahlmann, R., Bozkaya, Ö., Potel, S., Le Bayon, R., Nieto, F., 2012. The pioneer work of Bernard Kübler and Martin Frey in very low-grade metamorphic terranes: paleo-geothermal potential of variation in Kübler-Index/organic matter reflectance correlations. A review. Swiss J. Geosci. 105, 121–152.
Frey, M., 1987. Very low-grade metamorphism of clastic sedimentary rocks. In: Frey, M. (Ed.), Low-Temperature Metamorphism. Blackie and Son, Glasgow, UK, pp. 9–58.
Gat, J.R., Shemesh, A., Tziperman, E., Hecht, A., Georgopoulus, D., Basturk, O., 1996. The stable isotope composition of waters of the eastern Mediterranean Sea. J. Geophys. Res. 101, 6441–6451.
Görür, N., Tüysüz, O., Şengör, A.M.C., 1998. Tectonic evolution of the central Anatolian basins. Int. Geol. Rev. 40, 831–850.
Gündoğdu, M.N., Yalçın, H., Temel, A., Clauer, N., 1996. Geological, mineralogical and geochemical characteristics of zeolite deposits associated with borates in the Bigadiç, Emet and Kırka Neogene lacustrine basins, Western Turkey. Mineral. Deposita 31, 492–513.
Hemley, J.J., Montoya, J.W., Marinenko, J.W., Luce, R.W., 1980. Equilibria in the system Al_2O_3-SiO_2-H_2O and some general implications for alteration/mineralization processes. Econ. Geol. 75, 210–228.
Honty, M., Clauer, N., Šucha, V., 2008. Rare-earth elemental systematics of mixed-layered illite-smectite from sedimentary and hydrothermal environments of the Western Carpathians (Slovakia). Chem. Geol. 249, 167–190.
Inoue, A., 1995. Formation of clay minerals in hydrothermal environments. In: Velde, B. (Ed.), Origin and Mineralogy of Clays. Springer, Berlin, pp. 268–330.
Inoue, A., 2005. Formation of illite-smectite mixed-layer minerals in hydrothermally altered volcanic rocks: integration of geological, fluid chemical, isotopic, XRD, and TEM evidence at Kakkonda geothermal system. Clay Sci. 12, 13–20.
Inoue, A., Kitagawa, R., 1994. Morphological characteristics of illitic clay minerals from a hydrothermal system. Am. Mineral. 79, 700–711.
Inoue, A., Utada, M., 1991. Hydrothermal alteration in the Kamikita Kuroko mineralization area, northern Honshu, Japan. Mining Geol. Jpn. 41, 203–218.
Inoue, A., Kohyama, N., Kitagawa, R., Watanabe, T., 1987. Chemical and morphological evidence for the conversion of smectite to illite. Clay Clay Miner. 35, 111–120.
Inoue, A., Utada, M., Wakita, K., 1992. Smectite-to-illite conversion in natural hydrothermal systems. Appl. Clay Sci. 7, 131–145.
Kalkancı, Ş., 1974. Etüde geologique et petrochimique du sud de la region de Suşehri. Geochronologie du massif syenitique de Kösedağ (Sivas Turquie). These de doctoral de 3e cycle. L'universite de Grenoble (135 p).
Kalkancı, Ş., 1978. Geological and petrochemical investigation of the south of Suşehri. Geochronology of the Kösedağ syenitic massif (NE Sivas-Turkey). In: Turkish 32nd Scientific and Technical Congress, Abstracts, pp. 33–34.
Krumm, S., 1996. WINFIT 1.2: version of November 1996 (The Erlangen geological and mineralogical software collection) of "WINFIT 1.0: a public domain program for interactive profile-analysis under WINDOWS". XIII. Conference on Clay Mineralogy and Petrology, Praha, 1994. Acta Univ. Carol. Geol. 38, 253–261.
Kuşcu, I., Tosdal, R.M., Gençalioğlu-Kuşcu, G., Friedman, R., Ullrich, T.D., 2013. Late Cretaceous to middle Eocene magmatism and metallogeny of a portion of the southeastern Anatolian orogenic belt, east-central Turkey. Econ. Geol. 108, 641–666.
Longstaffe, F.J., Ayalon, A., 1990. Hydrogen-isotope geochemistry of diagenetic clay minerals from cretaceous sandstones, Alberta: evidence for exchange. Appl. Geochem. 5, 657–688.
Mao, J., Pirajno, F., Lehmann, B., Maocheng, L., Berzina, A., 2014. Distribution of porphyry deposits in the Eurasian continent and their corresponding tectonic settings. J. Asian Earth Sci. 79, 576–584.
Merriman, R.J., Frey, M., 1999. Patterns of very low-grade metamorphism in metapelitic rocks. In: Frey, M., Robinson, D. (Eds.), Low Grade Metamorphism. Blackwell Sciences Ltd., Oxford, UK, pp. 61–107.
Merriman, R.J., Peacor, D.R., 1999. Very low-grade metapelites: mineralogy, microfabrics and measuring reaction progress. In: Frey, M., Robinson, D. (Eds.), Low Grade Metamorphism. Blackwell Sciences Ltd., Oxford, UK, pp. 10–60.
Meunier, A., Velde, B., 1989. Solid solutions in l-S mixed layer minerals and illite. Am. Mineral. 74, 1106–1112.
Millot, G., 1970. Geology of Clays. Springer-Verlag, New York, p. 429.
Milodowski, A.E., Zalasiewicz, J.A., 1991. Redistribution of rare earth elements during diagenesis of turbidite/hemipelagite mudrock sequences of Llandovery age from Central Wales. Pp. 101124. In: Mort on, A.C., Todd, S.P., Haughton, P.D.W. (Eds.), Developments in Sedimentary Provenance Studies, 57. Geological Society of London (Special Publications).
Murakami, T., Inoue, A., Lanson, B., Meunier, A., Beaufort, D., 2005. Illite-smectite mixed-layer minerals in hydrothermal alteration of volcanic rocks: II. One-dimensional HRTEM structure images and formation mechanisms. Clay Clay Miner. 53, 440–451.
Nadeau, P.H., Wilson, J., McHardy, W.J., Tait, J.M., 1984a. Interparticle diffraction: a new concept for interstratified clays. Clay Miner. 19, 757–769.
Nadeau, P.H., Wilson, J., McHardy, W.J., Tait, J.M., 1984b. Interstratified clays as fundamental particles. Science 225, 923–925.
Odin, G.S., 1982. Interlaboratory standards for dating purposes. In: Odin, G.S. (Ed.), Numerical Dating in Stratigraphy. Wiley and Sons, Chichester, UK, pp. 123–149.
Ohr, M., Halliday, A.N., Peacor, D.R., 1994. Mobility and fractionation of rare earth elements in argillaceous sediments: implications for dating diagenesis and low-grade metamorphism. Geochim. Cosmochim. Acta 58, 289–312.
Parry, W.T., Jasumback, M., Wilson, P.N., 2002. Clay mineralogy of phyllic and intermediate argillic alteration at Bingham, Utah. Econ. Geol. 97, 221–239.
Parsapoor, A., Khalili, M., Mackizadeh, M.A., 2009. The behaviour of trace and rare earth elements (REE) during hydrothermal alteration in the Rangan area (Central Iran). J. Asian Earth Sci. 34, 123–134.
Pirajno, F., 2009. Hydrothermal Processes and Mineral Systems. Springer, Netherlands, p. 1250.
Reynolds Jr., R.C., 1985. NEWMOD: A Computer Program for the Calculation of One-Dimensional Diffraction Patterns of Mixed-Layered Clays. 8 Brook Rd, Hanover, New Hampshire, USA.

Reynolds Jr., R.C., 1994. WILDFIRE: A Computer Program for the Calculation of Three-Dimensional Powder X-Ray Diffraction Patterns for mica Polytypes and Their Disordered Variations. 8 Brook Rd, Hanover, New Hampshire, USA.
Savin, S.M., Lee, M., 1988. Isotopic studies of phyllosilicates. In: Bailey, S.W. (Ed.), Hydrous Phyllosilicates. Reviews in Mineralogy, 19. Mineralogical Society of America, Washington, D.C, pp. 189–223.
Sawai, O., Okada, T., Itaya, T., 1989. K-Ar ages of sericite in hydrothermally altered rocks around the Toyoha deposits, Hokkaido, Japan. Mining Geol. Jpn. 39, 191–204.
Şengör, A.M.C., Yılmaz, Y., 1981. Tethyan evolution of Turkey: a plate tectonic approach. Tectonophysics 75, 181–241.
Sheppard, S.M.F., Gilg, H.A., 1996. Stable isotope geochemistry of clay minerals. Clay Miner. 31, 1–24.
Sheppard, S.M.F., Nielsen, R.L., Taylor Jr., H.P., 1969. Oxygen and hydrogen isotope ratios of clay minerals from porphyry copper deposits. Econ. Geol. 64, 755–777.
Shikazono, N., Ogawa, Y., Utada, M., Ishiyama, D., Mizuta, T., Ishikawa, N., Kubota, Y., 2008. Geochemical behavior of rare earth elements in hydrothermally altered rocks of the Kuroko mining area, Japan. J. Geochem. Explor. 98, 65–79.
Środoń, J., 1984. X-ray powder diffraction identification of illitic minerals. Clay Clay Miner. 32, 337–349.
Środoń, J., Elsass, F., McHardy, W.J., Morgan, D.J., 1992. Chemistry of illite-smectite inferred from TEM measurements of fundamental particles. Clay Miner. 27, 137–158.
Sun, S.S., McDonough, W.E., 1989. Chemical and isotopic systematics of ocean basalts: implications for mantle composition and processes. In: Saunders, A.D., Norry, M.J. (Eds.), Magmatism in Ocean Basins, vol. 42. Geological Society of London, London, pp. 313–345.
Sverjensky, D.A., Hemley, J.J., D'Angelo, W.M., 1991. Thermodynamic assessment of hydrothermal alkali feldspar-mica-aluminosilicate equilibria. Geochim. Cosmochim. Acta 55, 989–1004.
Taylor Jr., H.P., 1979. Oxygen and hydrogen isotope relationships in hydrothermal mineral deposits. In: Barnes, H.L. (Ed.), Geochemistry of Hydrothermal Ore Deposits, 2nd ed. John Wiley and Sons, New York, pp. 236–272.
Taylor, S.R., McLennan, S.M., 1985. The Continental Crust: Its Composition and Evolution. Blackwell, Oxford, United Kingdom, p. 312.
Tillick, D.A., Peacor, D.R., Mauk, J.L., 2001. Genesis of dioctahedral phyllosilicates during hydrothermal alteration of volcanic rocks: I. The Golden cross epithermal ore deposit, New Zealand. Clay Clay Miner. 49, 126–140.
Uysal, I.T., Golding, S.D., 2003. Rare earth element fractionation in authigenic illite-smectite from late Permian clastic rocks, Bowen Basin, Australia: implications for physico-chemical environments of fluids during illitization. Chem. Geol. 193, 167–179.
Uysal, Ş., Bedi, Y., Kurt, İ., Kılınç, F., 1995. Geology of Koyulhisar (Sivas) Area. General Directorate of Mineral Exploration and Research (MTA), Report No: 9838 (120 p. Ankara (unpublished)).
Velde, B., 1977. Clays and Clay Minerals in Natural and Synthetic Systems. Elsevier, Amsterdam, p. 218.
Velde, B., 1985. Clay Minerals: A Physico-Chemical Explanation of Their Occurence. Elsevier (426 p).
Velde, B., Brusewitz, A.-M., 1986. Compositional variation in component layers in natural illite/smectite. Clay Clay Miner. 34, 651–657.
Weaver, C.E., Pollard, L.D., 1973. The chemistry of C1ay minerals. In: Developments in Sedimentology, 15. Elsevier, Amsterdam (213 pp).
Wohletz, K., Heiken, G., 1992. Volcanology and Geothermal Energy. University of California Press, Berkeley.
Wolde-Gabriel, G., Goff, F., 1989. Temporal relations of volcanism and hydrothermal systems in two areas of the Jemez volcanic field, New Mexico. Geology 17, 986–989.
Wolde-Gabriel, G., Goff, F., 1992. K/Ar dates of hydrothermal clays from core hole VC-2B, Valles caldera, New Mexico and their relation to alteration in a large hydrothermal system. J. Volcanol. Geotherm. Res. 50, 207–230.
Yan, Y., Tillick, D.A., Peacor, D.R., Simmons, S.F., 2001. Genesis of dioctahedral phyllosilicates during hydrothermal alteration of volcanic rocks: the Broadlands hydrothermal system, New Zealand. Clay Clay Miner. 49, 141–155.
Yeh, H.-W., 1980. D/H ratios and late stage dehydration of shales during burial. Geochim. Cosmochim. Acta 44, 341–352.
Yiğit, Ö., 2012. A prospective sector in the Tethyan Metallogenic Belt: geology and geochronology of mineral deposits in the Biga Peninsula, NW Turkey. Ore Geol. Rev. 46, 118–148.
Yılmaz, A., Okay, A., Bilgiç, T., 1985. Yukarı Kelkit Çayı yöresi ve güneyinin temel jeoloji özellikleri ve sonuçları. Maden Tetkik ve Arama Genel Müdürlüğü Rapor No: 7777, 124 s. Ankara (unpublished).
Ylagan, R.F., Altaner, S.P., Pozzuoli, A., 2000. Reaction mechanisms of smectite illitization associated with hydrothermal alteration from Ponza Island, Italy. Clay Clay Miner. 48, 610–631.
Zviagina, B.B., Drits, V.A., Środoń, J., McCarty, D.K., Dorzhieva, O.V., 2015. The illite-aluminoceladonite series: distinguishing features and identification criteria from X-ray diffraction and infrared spectroscopy data. Clay Clay Miner. 63, 378–394.
Zwingmann, H., Offler, R., Wilson, T., Cox, S.F., 2004. K-Ar dating of fault gouge in the northern Sydney basin, NSW Australia – implications for the breakup of Gondwana. J. Struct. Geol. 26, 2285–2295.